PNNL-16272
Revision 1

Pacific Northwest
National Laboratory
Operated by Battelle for the
U.S. Department of Energy

Potential Impacts of Leakage from Black Rock Reservoir on the Hanford Site Unconfined Aquifer: Initial Hypothetical Simulations of Flow and Contaminant Transport

VL Freedman

January 2008

Prepared for the U.S. Bureau of Reclamation
under an Interagency Agreement with the
U.S. Department of Energy
under Contract DE-AC05-76RL01830

PACIFIC NORTHWEST NATIONAL LABORATORY
operated by

BATTELLE
for the
UNITED STATES DEPARTMENT OF ENERGY
under Contract DE-AC05-76RL01830

Printed in the United States of America
Available to DOE and DOE contractors from the
Office of Scientific and Technical Information,
P.O. Box 62, Oak Ridge, TN 37831-0062;
ph: (865) 576-8401
fax: (865) 576-5728
email: reports@adonis.osti.gov

Available to the public from the National Technical Information Service,
U.S. Department of Commerce, 5285 Port Royal Rd., Springfield, VA 22161
ph: (800) 553-6847
fax: (703) 605-6900
email: orders@ntis.fedworld.gov
online ordering: http://www.ntis.gov/ordering.htm

PNNL-16272
Revision 1

Potential Impacts of Leakage from Black Rock Reservoir on the Hanford Site Unconfined Aquifer: Initial Hypothetical Simulations of Flow and Contaminant Transport

V. L. Freedman

January 2008

Prepared for the U.S. Bureau of Reclamation
under an Interagency Agreement with the
U.S. Department of Energy
under Contract DE-AC05-76RL01830

Pacific Northwest National Laboratory
Richland, WA 99352

Summary

Initial scoping calculations of the unconfined aquifer at the Hanford Site were carried out for the U.S. Bureau of Reclamation (USBR) to investigate the potential impacts on the Hanford unconfined aquifer that would result from leakage from the proposed Black Rock Reservoir to the west. Although impacts on groundwater flow and contaminant transport were quantified based on numerical simulation results, the investigation represented a qualitative assessment of the potential lateral recharge that could result in adverse effects on the aquifer. Because the magnitude of the potential leakage is unknown, hypothetical bounding calculations were performed. When a quantitative analysis of the magnitude of the potential recharge from Black Rock Reservoir is obtained, the hydrologic impacts analysis will be revisited.

The analysis presented in this report represents initial bounding calculations. A maximum lateral recharge (i.e., upland flux) was determined in the first part of this study by executing steady-state flow simulations that raised the water table no higher than the elevation attained in the Central Plateau during the Hanford operational period. This metric was selected because it assumed a maximum remobilization of contaminants that existed under previous fully saturated conditions.

Three steady-state flow fields were then used to analyze impacts to transient contaminant transport: a maximum recharge (27,000 acre-ft/yr), a no additional flux (365 acre-ft/yr), and an intermediate recharge case (16,000 acre-ft/yr). The transport behavior of four radionuclides, tritium, iodine-129, technetium-99, and uranium-238, was assessed for a 300 year simulation period with the three flow fields. .

Transient flow and transport simulations were used to establish hypothetical concentration distributions in the subsurface. Using the simulated concentration distributions in 2005 as initial conditions for steady-state flow runs, simulations were executed to investigate the relative effects on contaminant transport from the increased upland fluxes. Contaminant plumes were analyzed for 1) peak concentrations and arrival times at downstream boundaries, 2) the area of the aquifer contaminated at or above the drinking water standard (DWS), and 3) the total activity remaining in the domain at the end of the simulation. In addition to this analysis, unit source release simulations from a hypothetical tracer were executed to determine relative travel times from the Central Plateau.

The results of this study showed that increases in the lateral recharge had limited effects on regional flow directions but accelerated contaminant transport. Although contaminant concentrations may have initially increased for the more mobile contaminants (tritium, technetium-99, and iodine-129), the accelerated transport caused dilution and a more rapid decline in concentrations relative to the base case (no additional flux). For the low-mobility uranium-238, higher lateral recharge caused increases in concentration, but these concentrations never approached the DWS.

In this preliminary investigation, contaminant concentrations did not exceed the DWS study metric. With the increases in upland fluxes, more mass was transported out of the aquifer, and concentrations were diluted with respect to the case where no additional flux was considered (base case).

Contents

Figures

Tables

1.0 Introduction

This document provides initial bounding calculations that assess the potential hydrologic effects on groundwater flow and contaminant transport on the Hanford unconfined aquifer from the proposed Black Rock Reservoir, which is to be sited ~7.5 miles west of the Hanford Basin (Figure 1.1). Several potential effects are anticipated from an increase in the lateral recharge (i.e., upland flux) to the Hanford unconfined aquifer from the proposed reservoir. These include an increase in the water-table elevation, hydraulic gradients, and groundwater-flow velocities. If the leakage is large enough to raise the water table to the surface, perennial surface flow on the western boundary of the Hanford Site could also result. Impacts to existing contaminants include accelerated transport, and mobilization of contaminants in the vadose zone.

The U.S. Bureau of Reclamation (USBR) is charged with evaluating the effects associated with the proposed reservoir in Black Rock Valley. In keeping with this charge, the USBR has begun a series of numerical and field investigations to examine potential effects resulting from the construction of the reservoir, including the hypothetical numerical results presented in this report. Although the simulations are analyzed quantitatively, several simplifying assumptions are made that lend the results of the analysis to a qualitative assessment of effects. For example, only steady-state flow analyses were executed to examine effects on flow. Although transport analyses were transient, the mobilization of contaminants in

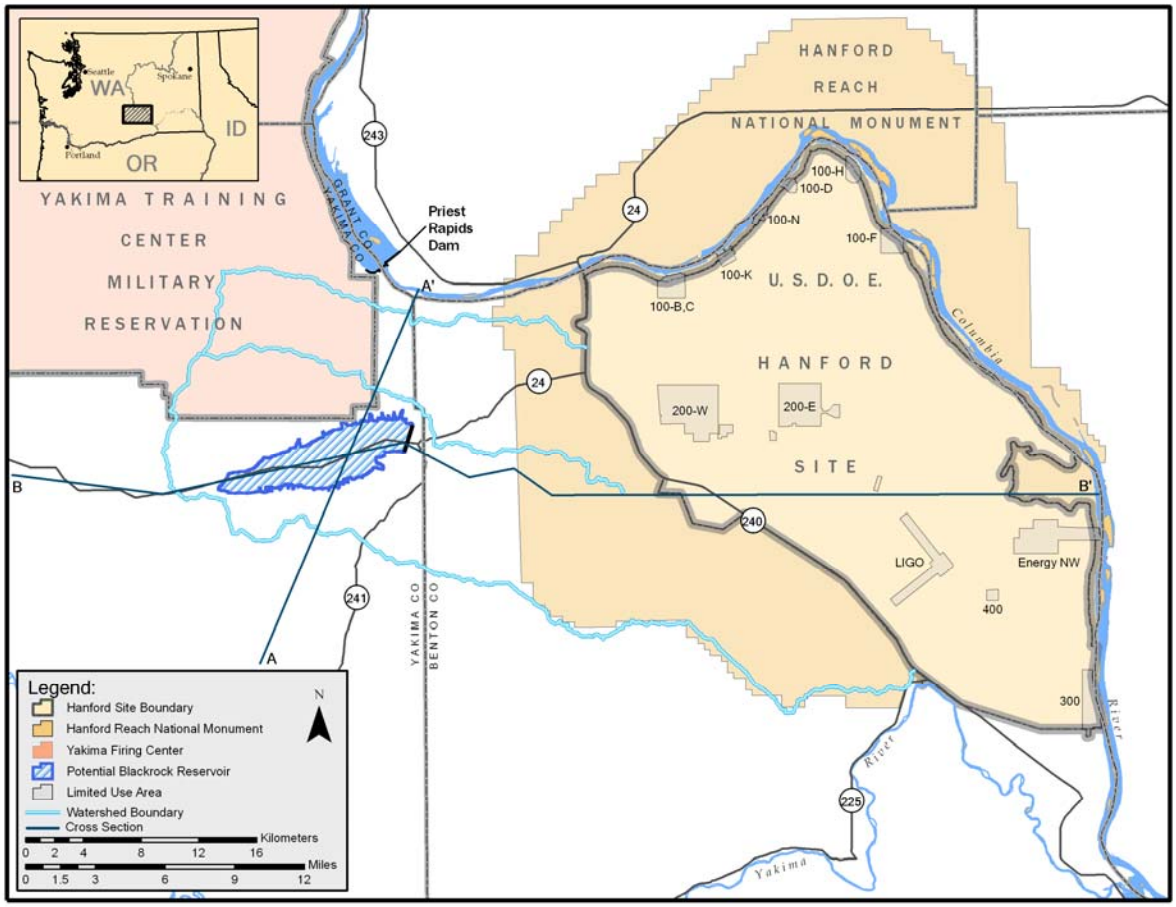

Figure 1.1. Proposed Location of Black Rock Reservoir West of the Hanford Site

the vadose zone could not be addressed with a saturated flow analysis. Even the magnitude of the potential leakage from the reservoir has not yet been quantified, and the potential subsurface pathways within basalt and sedimentary geologic formations are still under investigation. Because the results presented in this report are bounding calculations, once an analysis of the magnitude of the potential recharge is obtained, the effects on the unconfined aquifer will be re-evaluated.

In this report, initial scoping calculations were performed using the Hanford Site-Wide Groundwater Model (SGM) described in Thorne et al. (2006). The first objective of this analysis was to investigate a maximum potential lateral recharge (flux) that raised the water table to the historical levels attained during the Hanford operational period. The metric for the maximum recharge was selected because it represented a maximum remobilization of contaminants in the vadose zone that were previously under fully saturated conditions. This approach assumed no effect from continuing sources in the deep vadose zone that may have already migrated beneath the elevation of the maximum water table. The second objective was to evaluate effects for the maximum flux determined in the first part of the analysis. Effects on transport were analyzed for four radionuclides at Hanford, including tritium, iodine-129, technetium-99, and uranium-238.

This analysis focused on the hydrologic effects that increased lateral recharge may have on both groundwater flow and contaminant transport relative to a scenario in which no additional fluxes were assumed. Results from this analysis can be used to guide future investigations and provide a basis for management decisions on the feasibility of the proposed reservoir.

1.1 Background

The Hanford Site is a 560-square-mile complex in southeastern Washington State that has been operated since 1943 by the U.S. Department of Energy (DOE) and its predecessor agencies for the production of nuclear materials for national defense programs. Large volumes of radioactive, hazardous, and other wastes have been discharged to the subsurface, resulting in contaminant plumes in the vadose zone and groundwater. These infiltration events resulted in large water table changes and created significant groundwater mounds (in excess of 20 m) under waste management facilities in the central part of the site. Since the mission at the Hanford Site changed from weapons production to environmental restoration in 1988, the cessation of wastewater discharges has caused groundwater mounds to decline. If water levels continue to decline at their current rate of ~0.1 m in the 200 East and ~0.35 in the 200 West Areas (Hartman et al. 2006), groundwater mounds could dissipate within 30 years. However, the rate of groundwater decline is not expected to be linear, and the groundwater mounds beneath the Central Plateau may require much longer, perhaps hundreds of years, to completely dissipate. The ultimate goal of the restoration mission is to protect public health and safety and to mitigate and remediate environmental damage from exposure to the contaminants at Hanford. Milestones for cleanup at the Hanford Site have been established by the Tri-Party Agreement (TPA M-45-98-03).

Black Rock Valley is in a basalt syncline situated in the upper watershed of Dry Creek, part of the Greater Cold Creek drainage that includes the western portion of the Hanford Site. The Black Rock Reservoir is proposed to be sited in this location. The reservoir would be filled with water pumped from the Columbia River behind Priest Rapids Dam. The proposed reservoir would maintain 1.3 million acre-ft of water in active storage, which would inundate ~13.5 mi^2 if the maximum water surface elevation of 1778 ft is attained (Figure 1.2).

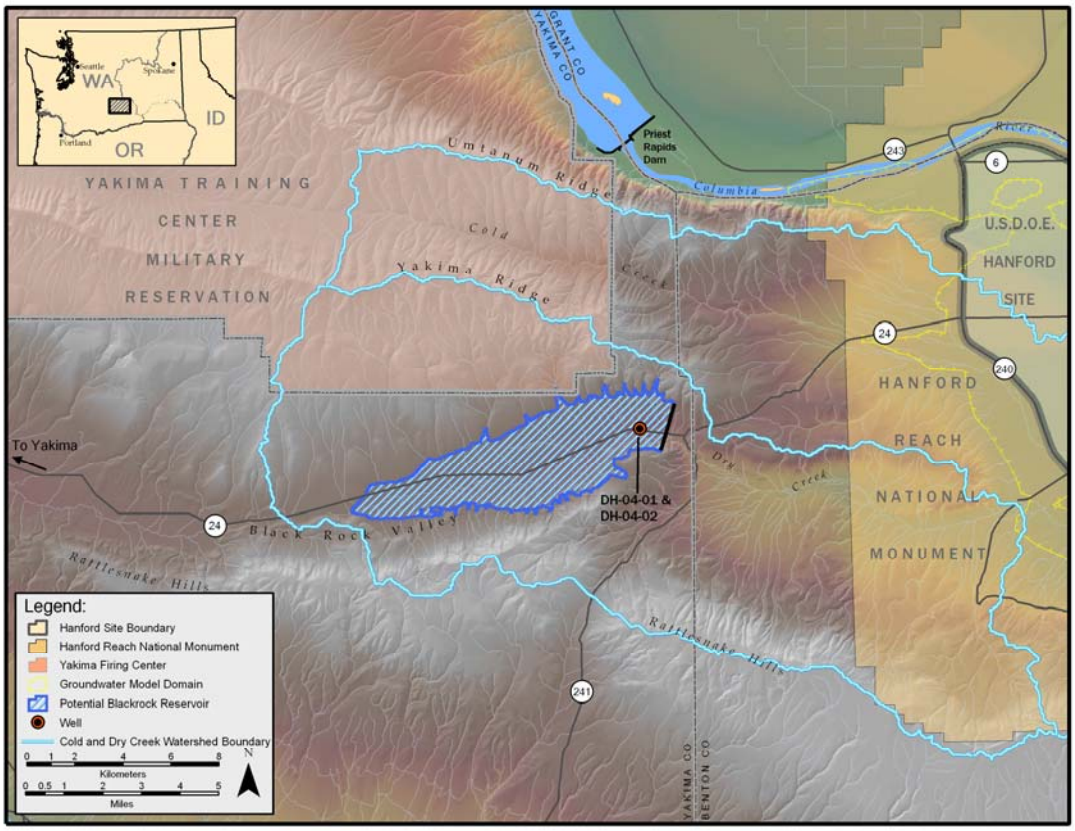

Figure 1.2. Proposed Size and Location of Black Rock Reservoir

There are three main pathways for leakage from the potential reservoir: 1) vertical flux through the base of the reservoir through the basalt contact, 2) lateral fluxes through the fractured and faulted basalt bedrock in the walls of the reservoir, and 3) vertical and lateral flow through the dam and geologic formations below the dam. Although the potential leakage pathways have been identified, considerable uncertainty exists for the leakage estimates from the reservoir. To date, only the potential for vertical leakage has been explored,(a) and further investigation is required to develop accurate estimates of leakage for all pathways and to translate these leakage estimates into downgradient fluxes entering the unconfined aquifer at Hanford.

1.2 Hanford Site-Wide Groundwater Model

Numerical simulations were carried out using CFEST (Coupled Fluid Energy and Solute Transport), a three-dimensional finite-element simulator for analyzing isothermal groundwater flow and solute transport problems (Freedman et al. 2005a, 2006). The CFEST simulator assumes a compressible fluid and porous medium, and flow is described with Darcy's law for advection. Solute transport considers decay, adsorption, and velocity-dependent dispersion. Infinite dilution is also assumed for coupling fluid flow and contaminant transport.

(a) Spane FA. 2004. "Results of the BY 2004 Borehole Hydrologic Field Testing Characterization Program, Black Rock Reservoir Study." Unpublished letter report, Pacific Northwest National Laboratory, Richland, Washington.

The SGM implemented in this study is based on a transient calibration of groundwater flow at the Hanford Site using the CFEST simulator. The SGM updated an earlier model (Cole et al. 2001) by using current geologic interpretations and extending the original hydraulic head observation data set (1944 through 1996) through the year 2004. Water fluxes for these facilities from the vadose zone to the unconfined aquifer used in this updated SGM calibration effort were developed with the vadose zone module of the System Assessment Capability (SAC) (Eslinger et al. 2006). In addition to new estimates of hydraulic conductivities and areal recharge, new estimates of boundary fluxes were obtained for Dry Creek and Cold Creek Valleys. The locations of these boundaries are shown in Figure 1.3, as are other important flow system boundaries for the Hanford unconfined aquifer. Fluxes between the unconfined aquifer and the underlying basalt confined aquifer were not considered in this calibration effort.

The potential leakage from Black Rock Reservoir was applied along the western boundary of the SGM and north of Rattlesnake Hills (Figure 1.3), as areal fluxes that are distributed laterally across a vertical cross section. Because alluvial sediments connect the reservoir site to Dry Creek Valley, nearly half of the total leakage estimate was applied at this location. There is also a potential for reservoir leakage to flow through the basalt to Cold Creek Valley. If leakage from the proposed reservoir recharges the confined aquifer, recharge between the two valleys is possible due to communication between the confined and unconfined aquifers. In this area, the Yakima thrust fault could provide a conduit for flow between aquifer systems (Vermeul et al. 2001). Lateral recharge to the unconfined aquifer could also raise the water table sufficiently such that sediments above the top of basalt become saturated.

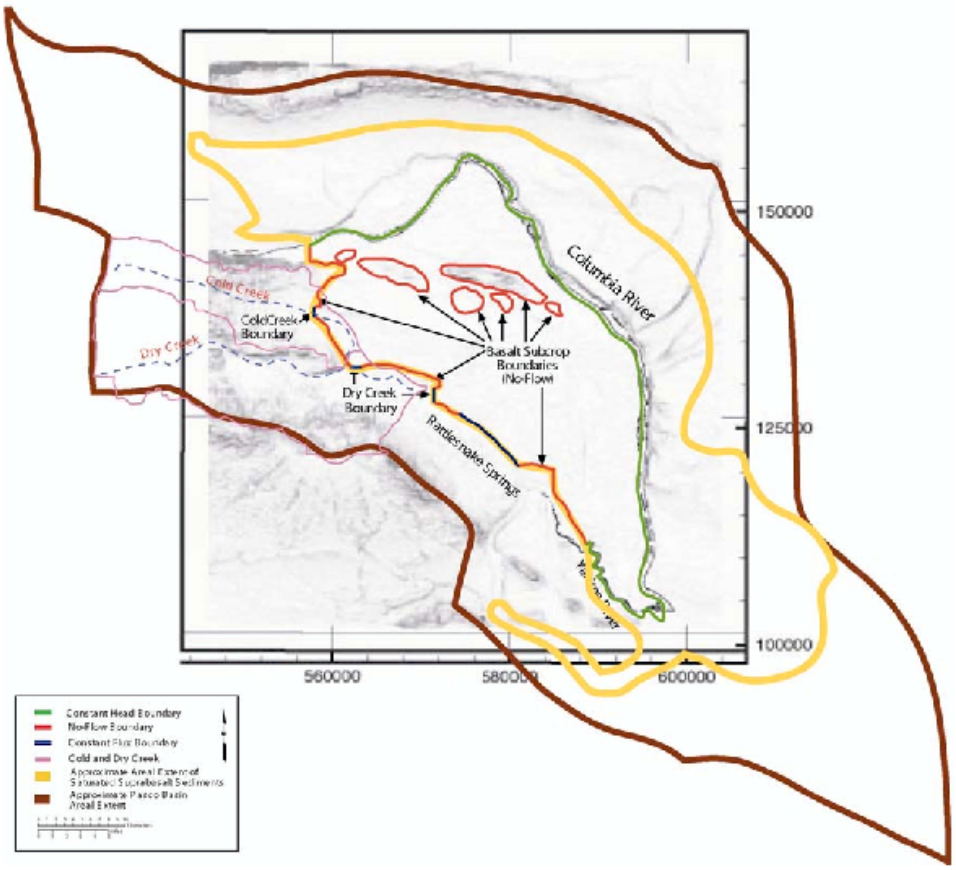

Figure 1.3. Hanford Site-Wide Model Domain Within the Pasco Basin Showing Flow System Boundaries (from Vermeul et al. 2001)

1.3 Approach

This report is divided into sections that generally follow the procedures used to execute the simulations. First, objectives are summarized, followed by a description of the methods used in the analysis. Next, a description of the flow and transport analyses is presented. A summary of results and preliminary conclusions that can be drawn from the numerical simulations are presented in the final section of the report.

Because flow and transport calculations in this analysis represent initial scoping calculations, steady-state flow was assumed because results could be obtained quickly. Several steady-state flow simulations were executed to determine the water table response to increases in the lateral recharge at the upland boundaries. Because the maximum increase in the water table during the Hanford operational period was in excess of 20 m in the 200 West Area in the Central Plateau and ~10 m in the 200 East Area (see Figure 1.1), the maximum lateral recharge to the groundwater-flow system was fixed at a level that would produce the maximum water table rise that occurred during Hanford operational period. Although any increase in the water-table elevation from present day levels would result in a rewetting of the unsaturated zone, this benchmark was used as an initial metric for determining a maximum recharge to the Hanford unconfined aquifer that returned the water table to Hanford operational levels. This metric was selected because it assumed no impacts from continuing sources in the deep vadose zone and a maximum remobilization of contaminants that existed under previous fully saturated conditions.

Once a threshold flux value was determined, transient flow and transport simulations were run to establish initial concentration distributions for the four radionuclides considered in this analysis. Simulated distributions were used because they could be obtained expeditiously and were adequate for performing an assessment of relative impacts on flow and transport. The transient simulations started in 1944 at the beginning of the operational period at Hanford and accounted for natural infiltration as well as operational discharges through 2005. Using the simulated concentration distributions in 2005 as initial conditions to steady-state flow runs, simulations were executed to investigate the potential impacts on contaminant transport from the increased upland fluxes. Transient solute transport was coupled to the steady-state flow regimes, and impacts were assessed for a 300-year simulation time period.

Because increases in upland fluxes were expected to primarily affect groundwater flow and contaminant transport in the Central Plateau, four contaminants (tritium, iodine-129, technetium-99, and uranium-238) in the 200 Areas were selected. These radionuclides were considered because their groundwater concentrations exceed the drinking water standard (DWS), and their distribution in the subsurface can be simulated with estimates of operational discharges from 1944 to the present. In addition, the transport behavior of each of the radionuclides is unique. For example, tritium travels conservatively but has a short half-life (~12 years). Technetium is also unretarded but has such a long half-life (2.13×10^5 years) that decay did not occur over the 300-year simulation. Both iodine-129 and uranium-238 adsorb to sediments. For these contaminants, mobility was defined through an equilibrium linear sorption coefficient (K_d), where the coefficient was set to 0.2 for iodine-129 and 0.6 for the more strongly sorbed uranium-238.

2.0 Technical Approach

This section describes the technical approach, rationale, and scope of work for the analysis presented in this report. Specifically, a description of the objectives, methods, and metrics associated with determining groundwater flow and contaminant transport effects from the potential influx from Black Rock Reservoir is presented. The technical approach for this modeling was developed based on the current understanding of site conditions. As the screening steps proceed and the evaluations of data further refine the extent of the potential impacts from the reservoir, adjustments will be made, if necessary, to the groundwater modeling analysis. An unsaturated zone analysis will also be needed to assess effects of contaminant mobilization in the deep vadose zone.

2.1 Objectives

The objectives of this analysis were to 1) estimate a lateral recharge (i.e., an upland boundary flux) that returned the groundwater table to maximum historical levels at the Hanford Site and 2) translate changes in flow and transport to impacts associated with exceeding DWS. Accordingly, the Hanford SGM (Thorne et al. 2006) was used to simulate flow and transport for existing conditions of the unconfined aquifer, as well as future leakage scenarios.

At this stage of the study, the potential leakage from Black Rock Reservoir has not yet been determined. Even though these simulations are subject to revision based on the results of future data collection and modeling analyses, the results presented in this report represent a range of potential effects from the reservoir. However, not all effects were addressed by the modeling. For example, the interaction between the unconfined and confined aquifer, transient effects on flow, and contaminant mobilization in the vadose zone were not considered in this investigation. In the transport analysis, effects were only quantified with respect to the DWS. Cumulative effects from exposure to multiple contaminants were ignored.

2.2 Overview of Modeling Analysis

To meet the specific modeling objectives, the general modeling approach included the following steps:

- Identify a maximum flux along the western boundary for the steady-state Hanford SGM that produced a water table rise no greater than 20 m in the 200 West Area and 10 m in 200 East Area.
- Simulate steady-state flow and transient contaminant transport at the maximum flux, no additional flux, and an intermediate flux estimates to evaluate impacts on
    - Flow velocities and directions
    - Contaminant concentration distributions exceeding the DWS
    - Peak concentrations and arrival times at downstream boundaries.

Although time-dependent impacts are anticipated from increases in the upland fluxes, steady-state flow was assumed due to long simulation times. The steady-state flow approach assumed that gradients (and velocities) immediately reached a maximum and that transport was accelerated with respect to a transient case.

Impacts associated with groundwater mounds beneath the Central Plateau were also not considered. Figure 2.1 shows the groundwater mounds that have formed through 1979. Currently, the groundwater mound beneath 200 East is estimated to be ~2 m higher than its pre-Hanford operational level and ~12 m higher in 200 West. These groundwater mounds were assumed to have dissipated in this analysis.

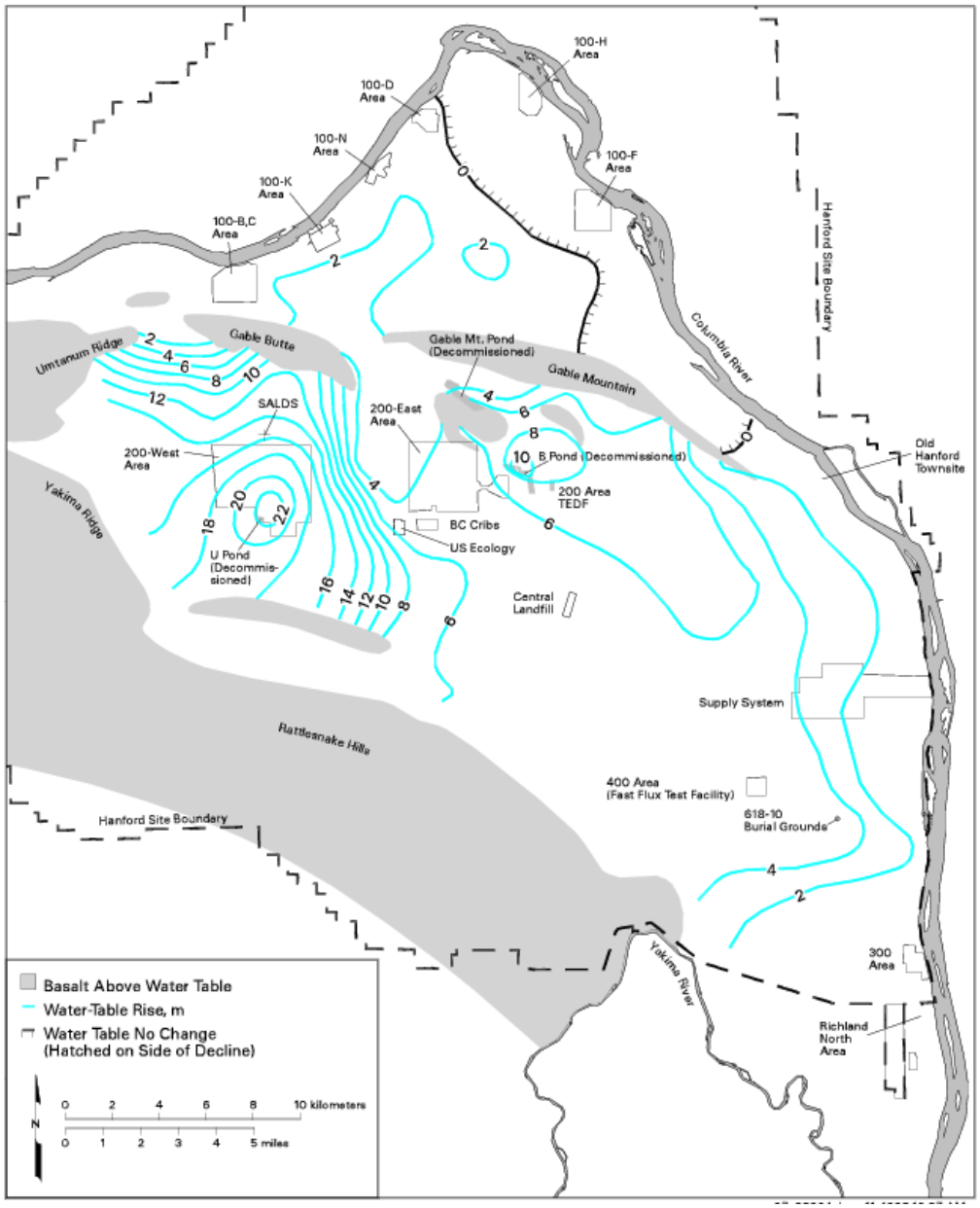

Figure 2.1. Changes in Water-Table Elevation Through 1979 (from Newcomer et al. 1998)

2.3 Groundwater Hydrology at Hanford

The Hanford Site lies within the Pasco Basin on the Columbia Plateau. Principal geologic units beneath the Hanford Site include, in ascending order, the Columbia River Basalt Group, the Ringold Formation, and the Hanford Formation (Newcomer et al. 1998). The unconfined aquifer forms the uppermost aquifer and is located in the Hanford and Ringold Formations. In some areas, the water table is below the bottom of the Hanford Formation and the unconfined aquifer is entirely within the Ringold Formation (Figure 2.2). The Hanford sands and gravels are unconsolidated and are much more permeable than the compacted and silty Ringold gravels. Clay and silt units and zones of natural cementation form low permeability zones within the Ringold Formation. The unconfined aquifer discharges primarily into the Columbia River. The amount of groundwater discharging into the river is a function of the local hydraulic gradient between the groundwater elevation adjacent to the river and the river-stage elevation.

Both confined and unconfined aquifers are present beneath the Hanford Site. The confined aquifers are generally isolated from the unconfined aquifer by dense rock that forms the interior of the basalt flows. However, interflow between the unconfined aquifer and the basalt-confined aquifer system is known to occur at faults that bring a water-bearing interbed into contact with other sediments or where the overlying basalt has been eroded to reveal an interbed (Newcomb et al. 1972). However, there is much uncertainty in quantifying this interaction (Vermeul et al. 2001). In the current model of the unconfined aquifer at the Hanford Site, the potential for interflow between the confined and unconfined aquifer systems is postulated to be very small relative to the other flow components estimated during the Hanford Site operational period. Therefore, the underlying basalt units were not included in the current SGM, and the bottom of the unconfined aquifer is treated as a no-flow boundary.

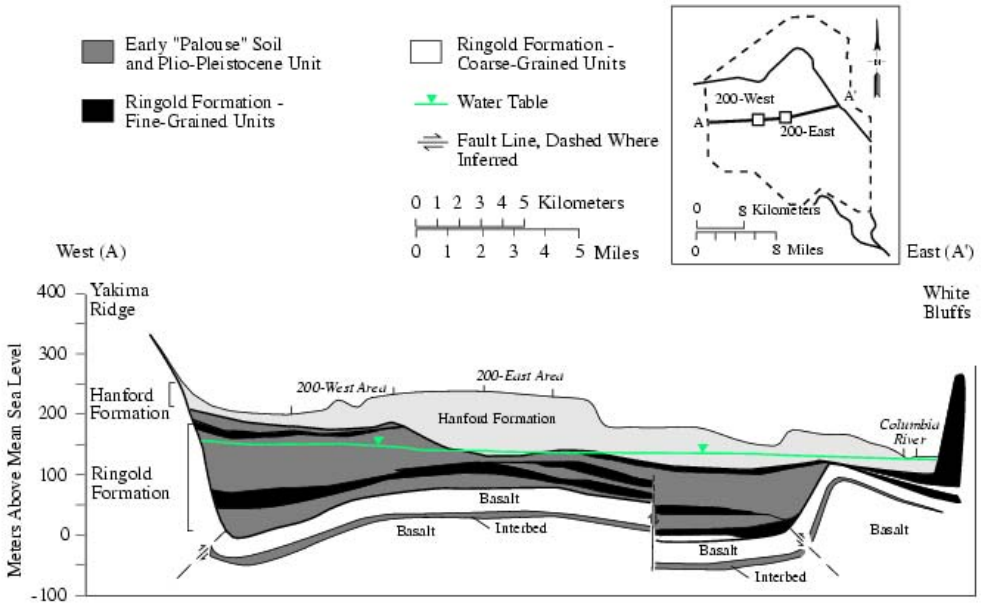

Figure 2.2. Geologic Cross-Section of the Hanford Site (from Newcomer et al. 1998)

2.3.1 Site-Wide Groundwater Model (SGM)

The SGM described in Thorne et al. (2006) was used in this study. It is based on a transient calibration of the unconfined aquifer at the Hanford Site using the CFEST simulator (Freedman et al. 2005a, 2006). The SGM updated an earlier model (Cole et al. 2001), by using current geologic interpretations and extending the original hydraulic head observation data set (1944–1996) through the year 2004. The transient calibration also included the discharge of large volumes of waste water to a variety of waste facilities. The vadose zone module of the SAC was used to provide these water and contaminant flux estimates to the groundwater (Eslinger et al. 2006). In addition to new estimates of hydraulic conductivities and areal recharge, new estimates of boundary fluxes, including Cold Creek and Dry Creek Valleys (Figure 2.3), were also revised.

Historically, plumes have migrated both north and east of the 200 Areas (see Figure 2.3) due to mounding caused by subsurface discharges. Flow simulations performed with the model described in Thorne et al. (2006) predict a dominant northerly future flow direction from the Central Plateau through

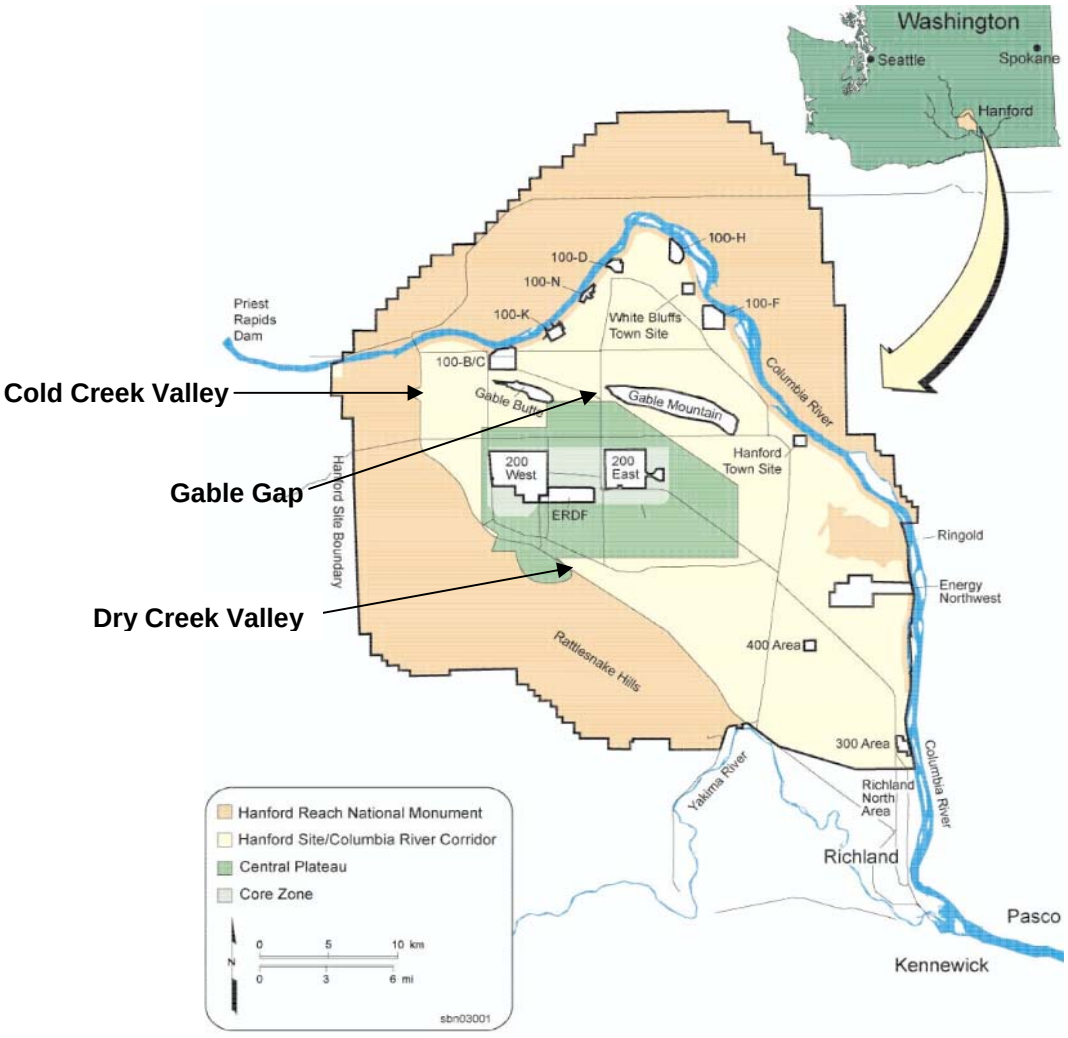

Figure 2.3. Map of Hanford Site

Gable Gap (between Gable Butte and Gable Mountain) by the time mounding dissipates and steady-state flow conditions are achieved. This result occurs, in part, because of constraints imposed on the conceptual model during calibration. Given the thin aquifer in Gable Gap and the continuing decline in the water table, future flows through the gap may be diverted eastward as the water table falls below the elevation of the top of the basalt.

There is a great deal of uncertainty surrounding the top of basalt elevation, and it is not yet possible to absolutely determine the future direction of groundwater flow in the Gable Gap area. Historically, high water tables have directed flow northward through the gap. Because this investigation was focused on relative impacts, the steady-state flow regimes that assumed a predominant northerly flow direction were considered adequate.

2.3.2 Distribution of Potential Leakage

The effects of leakage from the reservoir were studied by distributing the potential recharge among Dry Creek Valley (45%), the area just above and below Dry Creek Valley (27%), Cold Creek Valley (9%) and the basalt between these two alluvial channels (~19%) (see Figure 2.3). In Section 3.1, the distribution of the recharge, which was largely based on professional judgment, is discussed in more detail. The results were compared with base-case analyses in which only natural recharge (i.e., no additional flux) was applied at Dry Creek and Cold Creek boundaries. In the no-additional flux case, no flux is assumed along the basalt between the two alluvial valleys.

2.4 Maximum Lateral Recharge

To evaluate potential flow and contaminant transport impacts from the reservoir, the maximum potential leakage from Black Rock Reservoir should be considered. However, at this stage of the study, the potential leakage has not yet been identified. Hence, a maximum upland boundary flux to the Hanford Site was determined based on a maximum *acceptable* rise in the water table.

Because an increase in the lateral recharge would likely have the largest effect on transport from the Central Plateau (Figure 2.3), the most heavily contaminated area of the Site, the maximum change in the water table was determined based on maximum historical elevations in this geographic area. In 1979, groundwater mounds beneath the 200 West Area rose to more than 20 m above pre-Hanford operational levels (see Figure 2.1). In 1989, a ~10 m rise was attained in the water table beneath 200 East Area (Newcomer et al. 1998).

Since artificial subsurface discharges to these areas ceased in the early 1990s, groundwater mounds have begun to dissipate. In 200 West, current groundwater levels are ~12 m lower than maximum operational levels and ~2 m lower in 200 East (Hartman et al. 2006). Even though water-table elevations have not yet returned to their pre-operational levels, any increase in the water-table elevation from present day levels would result in a rewetting of the unsaturated zone. Contaminants in the vadose zone could then be mobilized even if the water table did not achieve the maximum water-table elevation attained historically. Although this metric assumed no effects from continuing sources, it represented a maximum remobilization for contaminants that existed under previously fully saturated conditions.

2.5 Selection Criteria for Contaminants

The 200 Areas are the most likely waste disposal area to be directly affected by changes in the lateral recharge at the upland boundaries. As a result, four major contaminants, tritium, iodine-129, technetium-99 and uranium-238, were selected for analysis. These radionuclides were considered because their groundwater concentrations currently exceed the DWS, and their distribution in the subsurface can be estimated by simulating operational discharges from 1944 to the present.

Earlier assessments predicted that the tritium plume beneath the 200 Area will be transported to the Columbia River in the near-term (~100 years), until the source is exhausted or until it decays below detection limits (Cole et al. 1997, Bryce et al. 2002). Predictions of the iodine-129 plume have shown that initial concentrations are not likely to fall significantly below current levels because of the radionuclide's long half-life, but will continue migrating toward and discharging to the Columbia River in the near-term. The technetium-99 plume poses a threat due to its conservative transport behavior and long half-life. By contrast, uranium-238 is strongly adsorbed to sediments, and current uranium plumes are not expected to migrate significantly from their current locations.

The transport behavior of each of the radionuclides is unique. For example, tritium travels conservatively but has a short half-life (~12 years). Technetium is also unretarded but has such a long half-life (2.13×10^5 years) that decay would not occur over the 300-year simulation period of interest. Both iodine-129 and uranium-238 adsorb to sediments. For these contaminants, mobility was defined through an equilibrium linear sorption coefficient (K_d), where the coefficient of 0.2 was assumed for iodine-129 and 0.6 for the more strongly sorbed uranium-238. These data are summarized in Table 2.1.

Table 2.1. Properties of the Contaminants

Radionuclide	Distribution Coefficient (K_d)	Retardation Coefficient (R)	Half-life ($t_{1/2}$, yr)	DWS (pCi/L)
Tritium (^{3}H)	0.0	1.0	1.23×10^{1}	20,000
Technetium-99 (^{99}Tc)	0.0	1.0	2.13×10^{5}	900
Iodine-129 (^{129}I)	0.2	2.0	1.57×10^{7}	1
Uranium-238 (^{238}U	0.6	5.0	4.46×10^{9}	27

2.6 Concentration Distribution Estimates

Because discharges to the subsurface have been estimated for 1944 to the present (Kincaid et al. 2004, Bryce et al. 2002), historical plumes can be simulated and predictions made on contaminant transport behavior. Although an exact match of contaminant plumes cannot be made to current conditions, the contaminant distributions could be used for assessing relative impacts due to changes in the flow field.

Simulations were executed from 1944 to the present to obtain contaminant concentration distributions for current conditions. The concentration distributions simulated in the year 2005 were then used as an initial condition to the three steady-state flow fields established by the different upland flux estimates. Water-table elevations differed among the three flow fields and the transient simulation that established

the initial concentration distribution in the subsurface. In the CFEST simulator, elements collapse to adjust to the calculated phreatic surface. All elements have a finite thickness (0.1 m) and an associated concentration. For the additional flux cases where the water table was higher than the transient water table computed in 2005, mass within the collapsed elements mixed with a larger volume of water when the element was expanded to adjust to the steady-state water table. The converse occurred for the base case, where mass mixed with smaller volumes of water due to elements collapsing to adjust to a lower phreatic surface.

Although contaminant transport predictions can be made for hundreds of thousands of years, nearer-term predictions of transport (~300 years) were used to assess the effects of increased fluxes to the Hanford aquifer. This time period was selected based on estimates that the tritium and iodine-129 plumes from the Central Plateau to the Columbia River will exceed the DWS for the next 150 to 300 years and that other contaminants will drop below the DWS within this same time period (DOE 2005).

2.7 Metrics for Impact Assessment

everal metrics were used to compare the no additional flux case with the different potential leak volumes from Black Rock Reservoir. These metrics quantified impacts of increased fluxes in terms of both flow and transport. For contaminated sites, potential impacts are typically viewed as harmful. In this analysis, the term is only used to describe change from a baseline condition, without a qualitative assessment of its harm or benefit.

The analysis of impacts presented in this report focuses on contaminant concentrations that exceed DWS. Although a complete analysis should account for cumulative impacts, for the initial scoping calculations presented in this report, effects are assessed in terms of a DWS for the individual contaminants. Peak concentrations and their corresponding arrival times are examined with respect to the DWS at downstream boundaries, which include the core zone and the Columbia River. Analyses of peak concentrations are commonly used for determining compliance for tank farm waste streams at Hanford (e.g., Zhang et al. 2004, Freedman et al. 2005b).

2.8 Downstream Boundaries

The downstream locations used to evaluate impacts in this analysis are based on future land use designations that support the cleanup mission at Hanford. Figure 2.3 shows the current planned future use designation at Hanford. Multiple uses of the Hanford Site are anticipated, including consolidating waste management operations in the Central Plateau, allowing industrial development in the eastern and southern portions of the Site, and increasing recreational access to the Columbia River (DOE 1999).

2.8.1 Core Zone

The core zone covers an area of 64.7 square kilometers (25 square miles) in the Central Plateau of the Hanford Site (see Figure 2.3). This geographical area, which encompasses all of the 200 East and West Areas, has been used heavily for fuel reprocessing, storage, disposal, and unplanned release of radioactive and nonradioactive wastes. Because this area is the most heavily contaminated on the Site, the DOE has

designated its future use as industrial-exclusive (DOE 2005). This designation allows for continued waste management operations within this area, which is needed to support the cleanup mission.

It is expected that groundwater contamination under the core zone will preclude beneficial use for the foreseeable future, which is at least the period of waste management and institutional controls (150 years). It is assumed that the tritium and iodine-129 plumes beyond the core zone boundary to the Columbia River will exceed the DWS for the next 150 to 300 years. It is expected that other groundwater contaminants will remain below or will be restored to drinking water levels outside the core zone (DOE 2005).

Currently, a buffer zone is defined that extends from the core zone to the Columbia River. This buffer zone should shrink to the core zone boundary over time. A period of 150 years has been identified as a reasonable time to switch from active to passive control outside the core zone.

2.8.2 Columbia River

The Columbia River, which is the second-largest river in the contiguous United States in terms of total flow, is the dominant surface-water body on the Hanford Site. This segment of the river contains 49 of the 51 miles of the Hanford Reach, the last unimpounded stretch of the Columbia River (HFSUWG 1992). Regionally, it is used for irrigation and recreation, which includes fishing, hunting, boating, water skiing, diving, and swimming. The river not only provides habitat for several species of endangered or threatened plants and animals but also is a source of drinking water for the City of Richland.

2.9 Flow Analysis

Steady-state flow fields were established for three different upland boundary fluxes: 1) the base case (no additional flux), 2) a maximum flux and 3) an intermediate estimate. Because transient effects on flow were ignored in this investigation, the focus of the flow analysis was on relative effects among the three different upland boundary conditions.

Changes in the upland boundary fluxes were first analyzed with respect to the effects on the flow field. Potentiometric surfaces were examined along with changes in the magnitude and direction of groundwater flow. Simulated velocities for the base case (i.e., no additional flux) scenario were directly compared with velocities simulated with higher flux estimates at the upland boundaries.

2.10 Transport Analysis

The transport analysis focused on the effects on contaminant concentration distributions associated with changes to the steady-state flow fields. For this reason, changes in peak concentrations and dispersal of the contaminant plume were used to examine relative impacts associated with increased fluxes at the upland boundaries. Hence, the analysis provided an ability to visualize the types of effects associated with the potential leakage from Black Rock Reservoir based on a concentration distribution that represented current conditions.

Three different metrics were then used to evaluate impacts: 1) area and volume of the contaminant plume at or above the DWS and 10 times the DWS, 2) peak concentrations and arrival times at the downstream boundaries (core zone and Columbia River), and 3) cumulative activity of the contaminants in the groundwater at the end of the 300-year simulation. Drinking water standards for each of the radionuclides simulated in this analysis are listed in Table 2.1.

In addition to the metric analysis, unit release scenarios for a hypothetical tracer were executed to determine differences in peak concentrations and arrival times to the downstream boundaries for each of the steady-state flow fields. The unit source analysis was also used to qualitatively examine differences in the areal extent of the plumes among the different flow fields. With no contaminant initially present, a unit source was injected as a pulse over a single time step into the subsurface at the center of 200 East and, in a separate simulation, into the subsurface at the center of 200 West Area. Time-dependent transport for each flow field was then simulated for 300 years, and relative differences in peak concentrations and arrival times were examined.

3.0 Flow Analysis

In the first part of this study, a maximum flux at the upland boundaries was determined using a steady-state flow analysis. These steady-state simulations were executed to determine the water table response to increases in the flux at the upland boundaries. Because the maximum increase in the water table during the Hanford operational period was ~20 m in the 200 West Area in the Central Plateau and ~10 m in 200 East (see Figure 2.1), a flux was determined at which the water table did not exceed these Hanford operational elevations. This benchmark was assumed to bound the maximum flux in these initial scoping calculations.

3.1 Lateral Recharge Distribution

Areal recharge (i.e., fluxes) in the CFEST simulator was applied at the element face and was distributed throughout a vertical stack of nodes. This boundary type distributes the total flux by the transmissivity of the vertical column. The current SGM applies a natural flux at Cold Creek of ~1700 acre-ft/yr. The flux at Dry Creek Valley is currently estimated at ~365 acre-ft/yr. For the base case (no additional flux) presented in this study, no-flow boundaries (i.e., zero-flux boundaries) were used along the western boundary between Cold Creek to Dry Creek Valleys.

The hypothetical recharge from Black Rock was applied to the model boundaries in addition to the fluxes already used to represent natural recharge to the two alluvial valleys. The potential leakage from Black Rock Reservoir, as described in Section 2.3.2, was distributed as an areal flux along the western boundary of the site between Cold Creek and Dry Creek Valleys (see Figure 3.1). Using professional judgment, this distribution was assigned based on potential subsurface pathways that may exist through both the alluvial channels and the basalt. Because Dry Creek Valley has the most direct hydraulic connection to the potential reservoir site, the majority of the flux (45%) was applied directly to this location in the SGM. As shown in Figure 3.1, only four surface nodes (3 elements) represent Dry Creek. For a smoother flux distribution, 14% of the flux was also applied to the vertical stack of elements represented by the three surface nodes above Dry Creek and 13% to the vertical stack of elements represented by the three surface nodes below it.

Because Cold Creek Valley may also be hydraulically connected to the potential reservoir, 9% of the total flux was applied at this location. If leakage from the proposed reservoir recharges the confined aquifer, recharge between the two valleys is possible due to communication between the confined and unconfined aquifers. In this area, the Yakima thrust fault could provide a conduit for flow between aquifer systems (Vermeul et al. 2001). Lateral recharge to the unconfined aquifer could also raise the water table sufficiently that sediments above the top of basalt become saturated.

Between the two valleys, there is a potential for recharge due to leakage to the confined aquifer and upward flux from the confined aquifer to the unconfined aquifer. Increased leakage could also raise the water table sufficiently that sediments above the top of basalt become saturated. The basalt between the two alluvial valleys received 19% of the total flux by distributing 1% of the flux to each vertical stack of elements between Cold Creek and Dry Creek Valleys (see Figure 3.1).

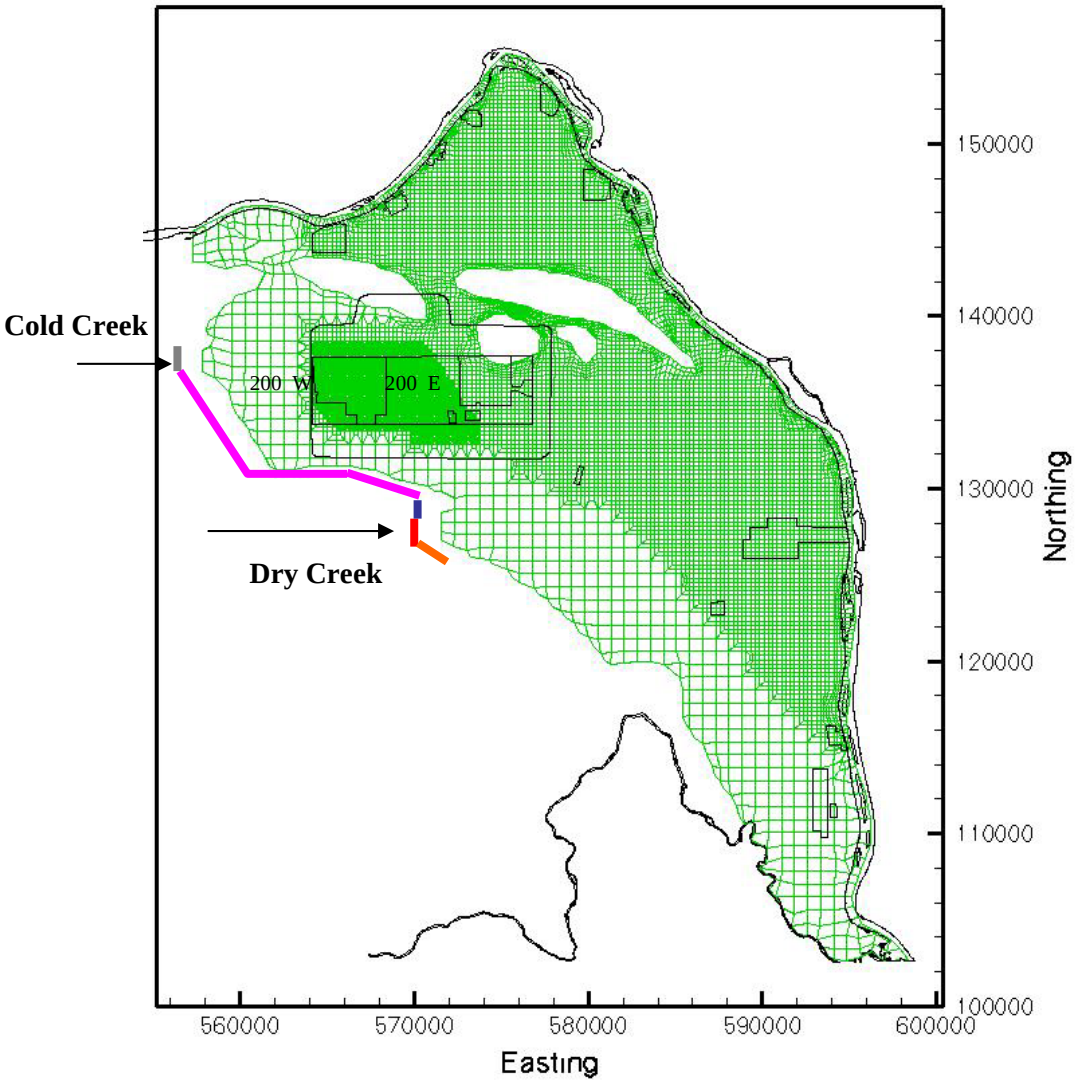

Figure 3.1. Percent Distribution of the Total Flux from Potential Leakage from Black Rock Reservoir as Implemented on the Hanford SGM Grid. Elements along the gray line at Cold Creek receive 9%; elements along the pink line, 19%; elements along the blue line, 14%; elements along the red line at Dry Creek, 45%; and elements along the orange line, 13%.

3.2 Head Distributions from Steady-State Simulations

In the sections that follow, results from three steady-state head distributions are presented. These represent the base case (no additional flux) and the maximum and intermediate flux resulting from leakage fro m the potential reservoir. Streamtraces are also discussed to demonstrate differences among all the cases in flow directions caused by increases in the upland boundary fluxes.

3.2.1 No Additional Flux Case

Shown in Figure 3.2 is the steady-state head distribution for the base case (no additional flux). This scenario used the natural recharge estimates at Cold Creek and Dry Creek Valleys for the calibrated SGM. Streamtraces in Figure 3.2 show that groundwater flowed northward through Gable Gap from the Central Plateau and discharged into the northern reach of the Columbia River.

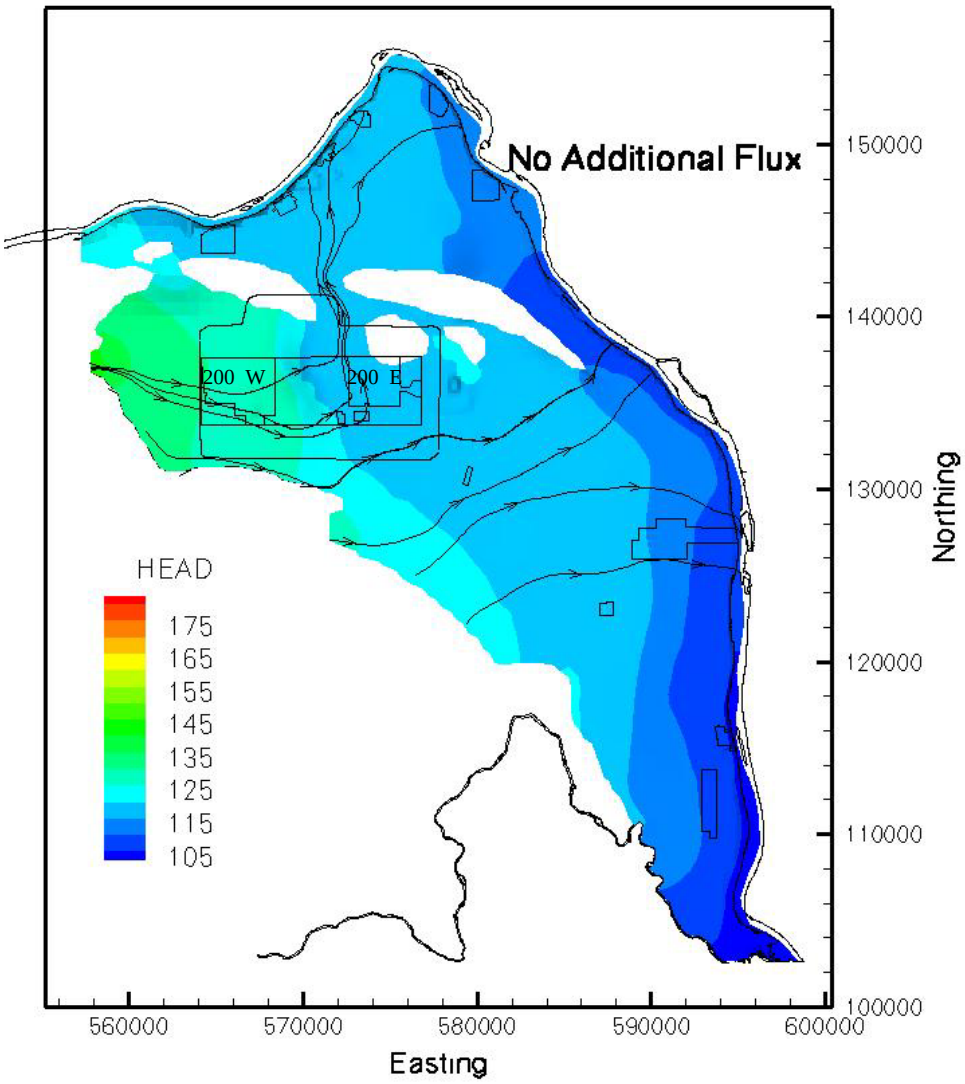

Figure 3.2. Steady-State Head Distribution for the Base Case Scenario

3.2.2 Maximum Recharge

Using the maximum historical rise in the water table at the 200 Areas as an upper bound, several steady-state flow simulations were run to identify a maximum flux that did not exceed this maximum change in water-table elevation. A flux of 27,000 acre-ft/yr was identified as a maximum flux that produced a ~20 m rise in head at 200 West Area and a ~7 m rise in head at 200 East (Figure 3.3).

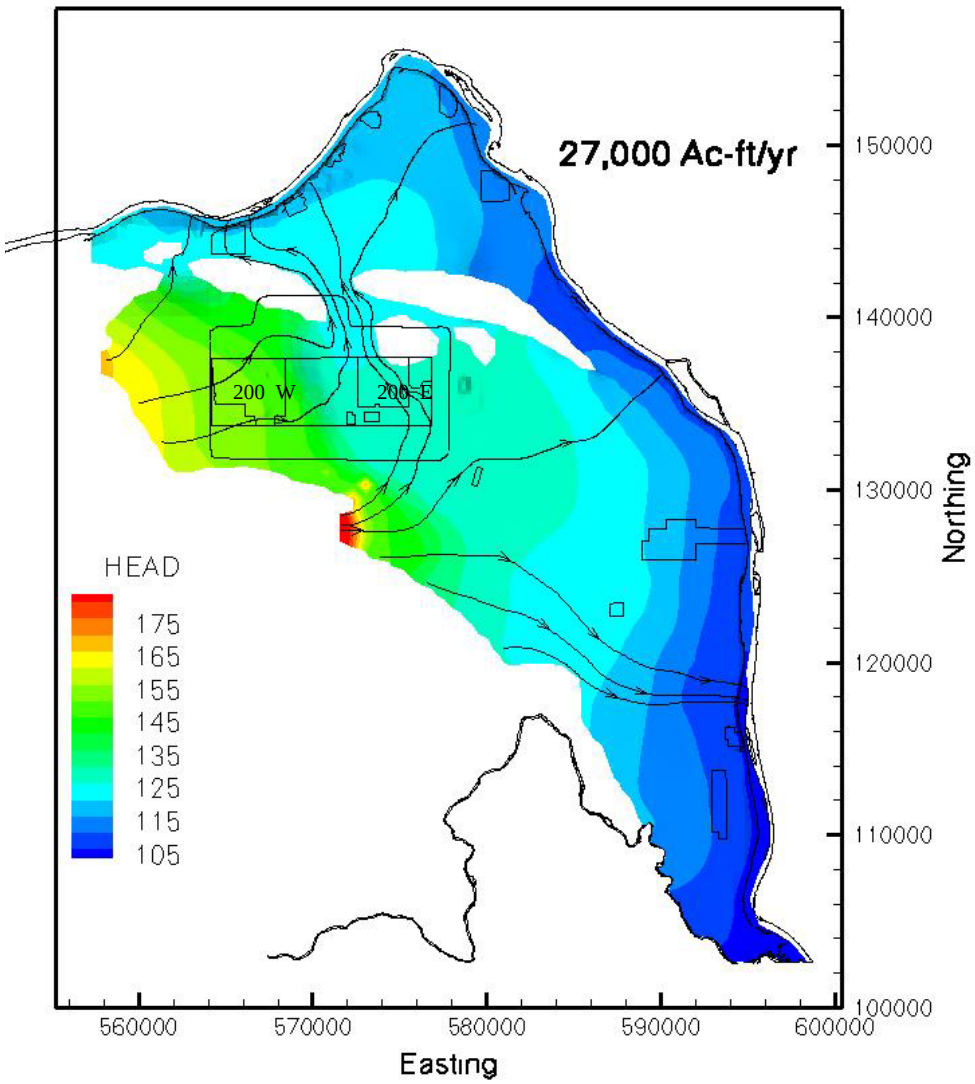

Figure 3.3. Steady-State Head Distribution Resulting from an Increase in the Upland Boundary Fluxes of 27,000 acre-ft/yr

A larger increase in the water table at 200 West resulted from its proximity to the upland flux boundary and to the low saturated hydraulic conductivities associated with the Ringold Formation (e.g., tens of meters per day). In 200 East, the saturated thickness lies within the Hanford Formation, where hydraulic conductivities in some areas can be on the order of thousands of meters per day. Additional influx of water to this area caused less mounding because water could be more easily transported through the conductive sediments.

Because the majority of the potential flux from Black Rock Reservoir was applied at Dry Creek Valley, the water table was highest at this location. Currently, this area in the SGM, which has very limited information about hydraulic properties of local hydrogeologic units, is represented with the Ringold Formation with hydraulic conductivities ~10 m/day. Recent work on alternative conceptual models for the Hanford Site has shown that Ringold sediments along the western edge of the Pasco Basin may be dominated by alluvial fan deposits and are expected to have higher conductivity (Vermeul et al.

2003). The conductivity of these sediments is important in controlling flow from recharge areas on the western boundary. Higher hydraulic conductivity would permit a faster influx of water and decrease both the hydraulic gradient and estimates of hydraulic head. With a total flux of 27,000 acre-ft/yr, the water-table elevation at Dry Creek was estimated at ~185 m, approximately 20 m higher than the ground surface (Figure 3.4). The gradient, however, dropped quickly and was at the ground surface at the adjacent element, a distance of 750 m. Given that there is uncertainty associated with the hydraulic conductivity estimates at Dry Creek, the rise in the water table at Dry Creek was likely overestimated. Hence, the initial scoping calculations focused on the impacts to the water table in the Central Plateau, and the boundary flux estimate of 27,000 acre-ft/yr was considered acceptable for evaluating impacts on flow and transport from the Central Plateau.

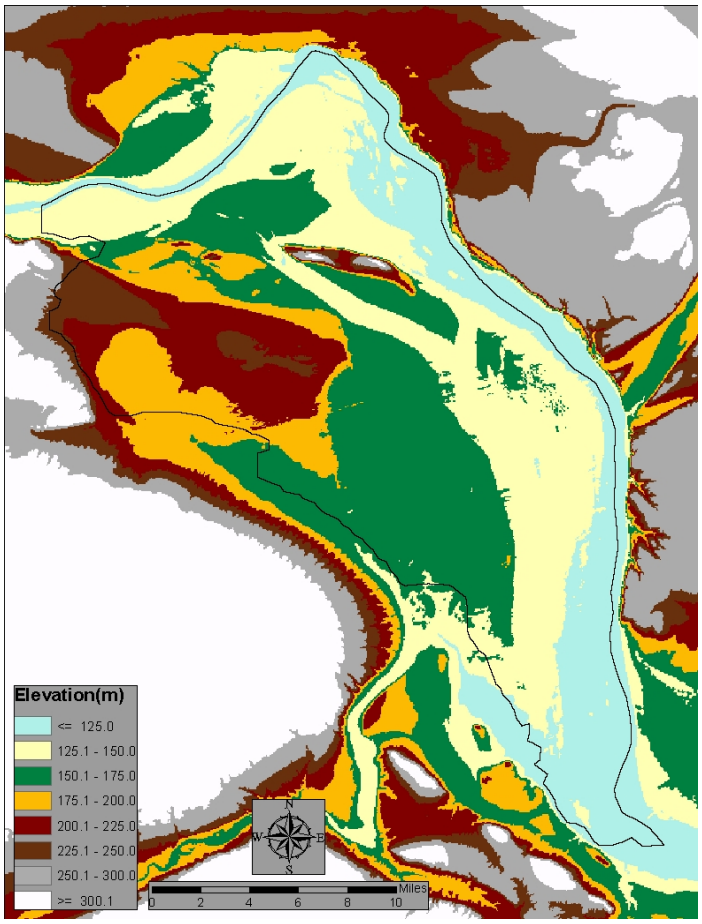

Figure 3.4. Surface Elevations of the Hanford Site Within the Pasco Basin

Streamtraces shown in Figure 3.3 demonstrate that regional flow directions are largely unaltered by the increase in the upland fluxes (see Figure 3.2). Flow paths from the Central Plateau exhibited only small changes in the southern part of 200 West. Groundwater from Dry Creek, however, showed more significant changes in flow direction. In the base case scenario, groundwater from Dry Creek Valley flowed predominately eastward toward the Columbia River. With an additional 27,000 acre-ft/yr flowing into the unconfined aquifer, groundwater from north of Dry Creek flowed northward through Gable Gap, whereas in the southern end of Dry Creek, eastward flow predominated. South of Dry Creek along Rattlesnake Hills, the additional flux caused more southerly flow paths than in the base case scenario.

3.2.3 Intermediate Recharge

The natural boundary recharge estimate at Dry Creek is ~365 acre-ft/yr. Because this flux was estimated during calibration, its value is inextricably tied to the hydraulic conductivity distribution and surface recharge estimates in the current SGM. Waichler et al. (2004) estimated the flux at Dry Creek at ~5000 acre-ft/yr, more than 10 times the calibrated value. Given the low estimate in the current SGM, the Waichler et al. (2004) estimate was used as a lower bound in selecting an intermediate boundary flux value. This intermediate flux was taken as the average between 5,000 and 27,000 acre-ft/yr. The steady-state head distribution with a total additional boundary flux of 16,000 acre-ft/yr is shown in Figure 3.5. At Dry Creek, the groundwater table is at the ground surface.

Streamtraces shown in Figure 3.5 demonstrate the same trends found in the 27,000 acre-ft/yr flux case (Figure 3.3). Like the maximum recharge case, groundwater from the Dry Creek flowed both north and east. South of Dry Creek along Rattlesnake Hills, the intermediate recharge estimate also caused the same southerly flow paths exhibited by the maximum recharge scenario.

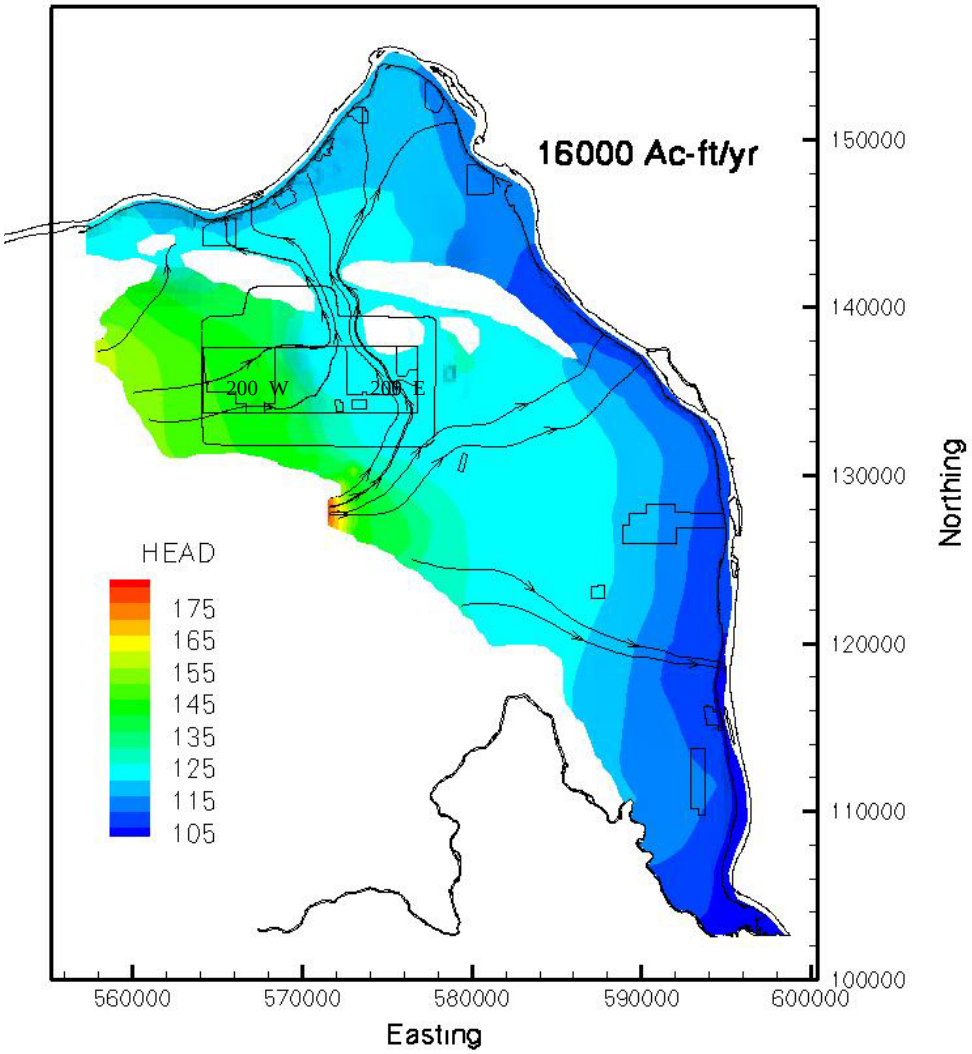

Figure 3.5. Steady-State Head Distribution Resulting from an Increase in the Upland Boundary Fluxes of 16,000 acre-ft/yr

3.3 Effects on Groundwater Flow Velocity

With the additional influx at the upland boundaries and subsequent increases in the hydraulic gradient, groundwater-flow velocities increased relative to the base case. Since the X and Y velocities determine lateral flow directions, these are quantified relative to the base case.

Shown in Figure 3.6 are the relative X and Y velocities for the 16,000 acre-ft/yr and 27,000 acre-ft/yr flow fields. In the Central Plateau, the average velocity for the Hanford and Ringold formations increased by a factor of ~13 and ~20 for the 16,000 and 27,000 acre-ft/yr cases, respectively. In the area north of Gable Gap, the relative change in velocities was higher at ~26 and ~38 times the value in the base case for the 16,000 and 27,000 acre-ft/yr cases, respectively. In the area east of Rattlesnake Hills, flow velocities were also affected, with the average relative velocities increasing by ~21 and ~26 times for the 16,000 and 27,000 acre-ft/yr cases, respectively.

The largest changes in velocities occurred in the Hanford formation. This is observed in Figure 3.6, which shows the highest velocity changes in 200 East, Gable Gap, and a localized region east of Rattlesnake Hills. Both the higher and intermediate flux cases showed similar trends, with the highest flux case resulting in larger velocity changes than in the intermediate flux case.

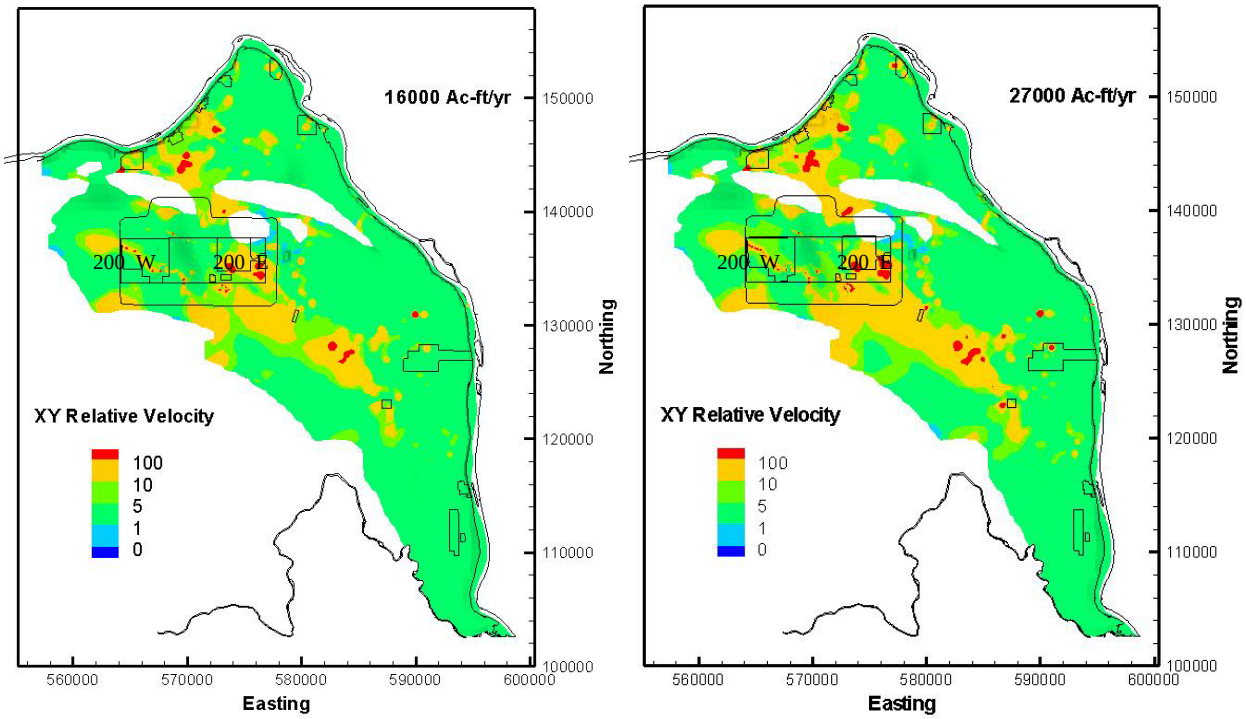

Figure 3.5. X-Y Flow Velocities Relative to Base Case for a) 16,000 acre-ft/yr and b) 27,000 acre-ft/yr

4.0 Transport Analysis

Two types of transport analyses were performed to evaluate the effects of increases in the upland boundary fluxes. The first analysis was based on estimates of current concentration distributions obtained from simulations of both natural recharge and operational water and contaminant discharges from 1944 through the present. These simulations established the initial conditions for the four radionuclides considered in this analysis (tritium, iodine-129, technetium-99 and uranium-238). Using the simulated concentration distributions in 2005 as initial conditions to steady-state flow runs, simulations were executed to investigate the potential impacts on contaminant transport from the increased recharge. Transient solute transport was coupled to steady-state flow regimes for a 300-year simulation time period. Because each contaminant was simulated separately, 12 simulations were executed to examine contaminant transport impacts for each of the four radionuclides.

In a second transport analysis, unit release scenarios for a hypothetical tracer were executed to determine differences in peak concentrations and arrival times to the downstream boundaries for each of the steady-state flow fields. This analysis was performed to 1) assess contaminant spreading when no solutes were initially present and 2) determine travel times to the selected boundaries from the 200 Areas. This analysis was carried out by injecting a unit source as a pulse over a single time step (1 year) and then analyzing peak-to-peak concentrations at the boundaries. The tracer was assumed to be unretarded and not subject to radioactive decay. Two simulations were executed for each flow field, one in which the contaminant originated from the center of 200 West, and one in which the starting location was at the center of 200 East. Time-dependent transport for all six simulations was simulated for 300 years, and relative differences in peak concentrations and arrival times were evaluated.

4.1 Initial Concentration Distributions

Simulated contaminant distributions at the top of the water table surface in the year 2005 are shown in Figures 4.1 and 4.2 for each of the four radionuclides. Consistent with field observations, these predicted concentration distributions demonstrate that DWS are exceeded within the core zone for all four contaminants (Hartman et al. 2006). With the exception of uranium-238, the radionuclides exceeded the DWS outside the core zone boundary as well. Although the steady-state flow-fields predicted northerly flow through Gable Gap, the transient flow field used to simulate these concentration distributions directed groundwater in both easterly and northerly flow directions.

The concentration distributions shown in Figures 4.1–4.2 were used as an initial concentration condition to each of the steady-state flow fields. After 300 years of simulation, differences in peak concentrations at the boundaries, area of the aquifer contaminated at the DWS, and the total activity remaining in the simulation domain were analyzed for the three different flow fields.

4.1.1 Peak Concentrations

Peak concentrations and arrival times were identified at the core zone and Columbia River boundaries for each contaminant in each of the three steady-state flow fields. Figure 4.3 identifies peak locations for each of the four radionuclides. In all cases, except for technetium-99, the location of the peak concentration was dependent on the initial concentration distribution, and not the magnitude of upland fluxes. For

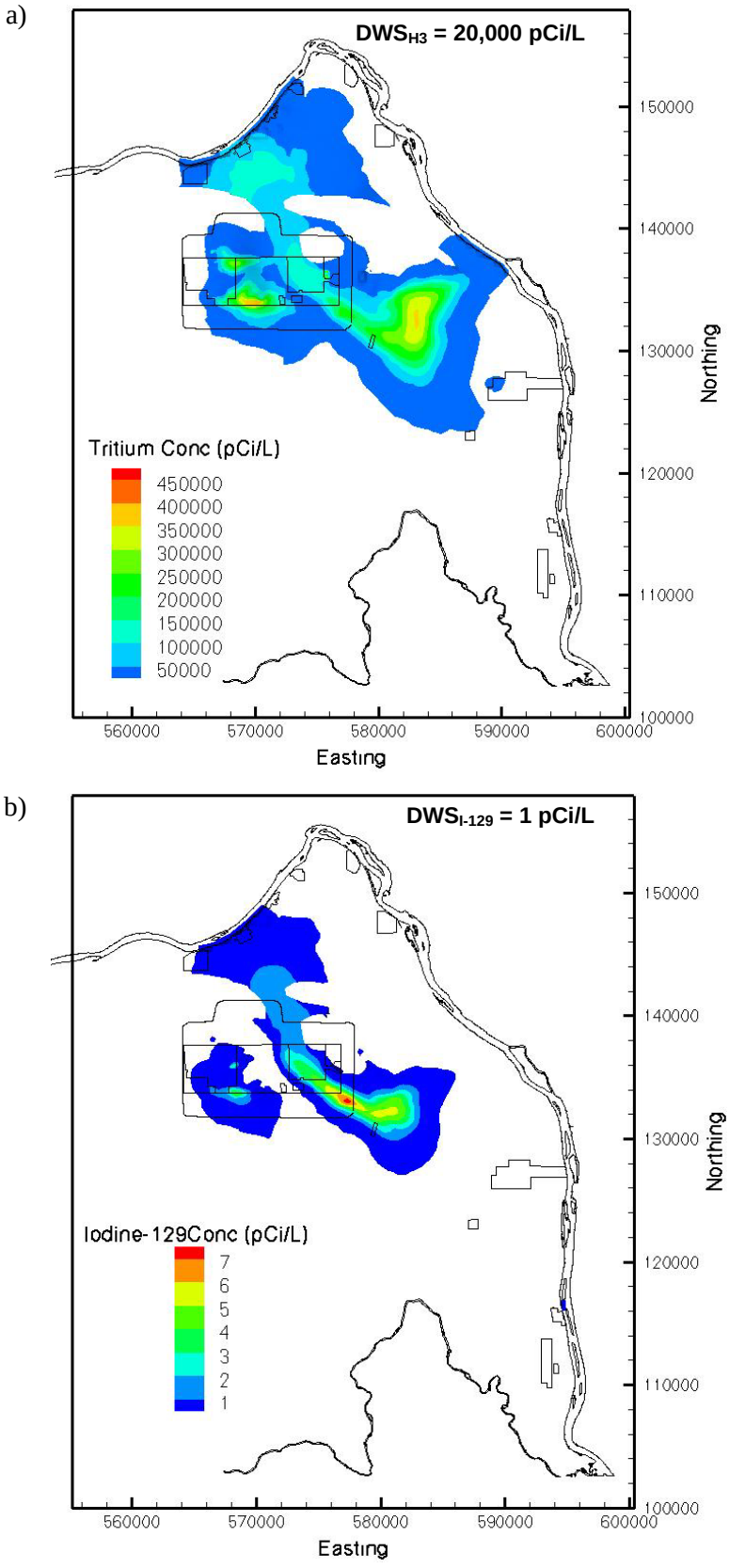

Figure 4.1. Simulated Concentration Distributions in the Year 2005 for a) Tritium and b) Iodine-129

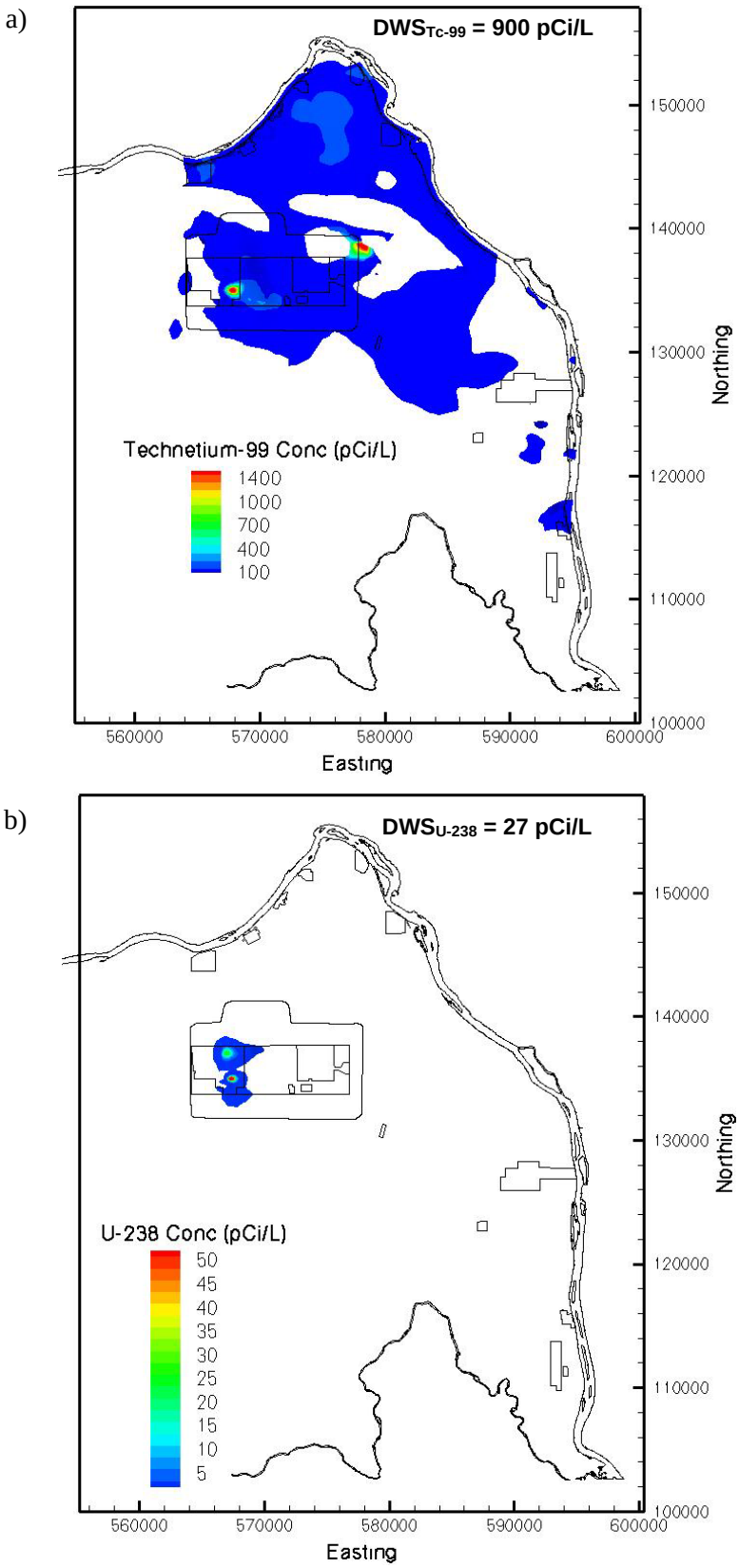

Figure 4.2. Simulated Concentration Distributions in the Year 2005 for a) Technetium-99 and b) Uranium-238

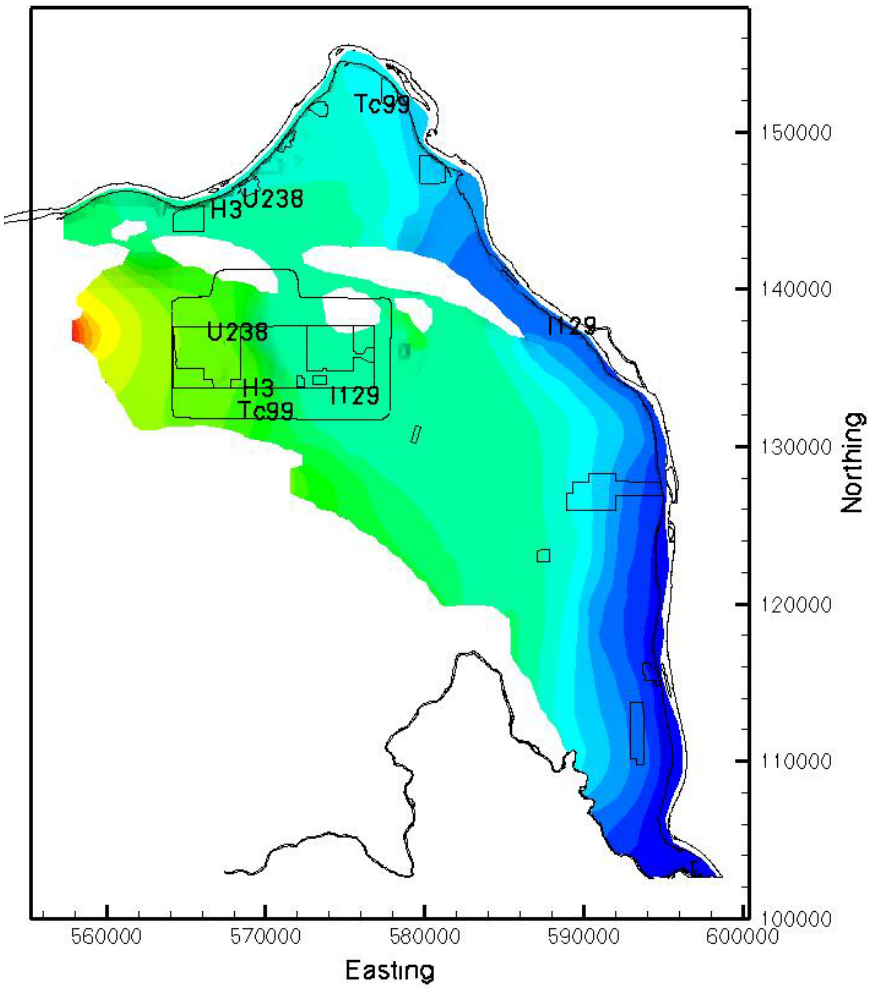

Figure 4.3. Peak Concentrations at the Core Zone and Columbia River Boundaries

technetium-99, however, the base case (no additional flux) peak occurred at the upper right corner of the core zone boundary near one of two high-concentration zones (see Figure 4.2). For the other two flux cases, the peak occurred just south of the high concentration zone in the 200 West Area. Because the increase in upland fluxes accelerated transport of technetium-99 from 200 West, the peaks along the southern boundary of the core zone for these two cases were higher than the peak in the base case. For consistency, the technetium-99 peak concentration at the core zone for the base case was analyzed at the same location as the other flux scenarios.

4.1.1.1 Results at Core Zone

Tables 4.1–4.4 report the peak concentrations and arrival times at the core zone for each of the contaminants. Also reported in these tables are their relative peak concentrations and differences in arrival times. With the exception of uranium-238, peak concentrations at this near-field boundary were highest in the year 2005 and exceeded the DWS. Breakthrough curves shown in Figures 4.4 and 4.5 show that as upland fluxes were increased the contaminants were diluted. Hence, the primary impact from a

Table 4.1. Peak Concentrations and Arrival Times at the Core Zone Boundary for Tritium. Relative peaks and arrival time differences are with respect to the base case (no additional flux).

Case	Peak Concentration (pCi/L)	Arrival Time (yr)	Relative Peak	Arrival Time Difference
No Additional Flux	31,000	2005	–	–
16,000 Acre-ft/yr	30,300	2005	0.98	0
27,000 Acre-ft/yr	30,000	2005	0.97	0

Table 4.2. Peak Concentrations and Arrival Times at the Core Zone Boundary for Iodine-129. Relative peaks and arrival time differences are with respect to the base case (no additional flux).

Case	Peak Concentration (pCi/L)	Arrival Time (yr)	Relative Peak	Arrival Time Difference
No Additional Flux	6.93	2005	–	–
16,000 Acre-ft/yr	6.57	2005	0.95	0
27,000 Acre-ft/yr	6.39	2005	0.92	0

Table 4.3. Peak Concentrations and Arrival Times at the Core Zone Boundary for Technetium-99. Relative peaks and arrival time differences are with respect to the base case (no additional flux).

Case	Peak Concentration (pCi/L)	Arrival Time (yr)	Relative Peak	Arrival Time Difference
No Additional Flux	150	2005	–	–
16,000 Acre-ft/yr	144	2005	0.96	0
27,000 Acre-ft/yr	142	2005	0.95	0

Table 4.4. Peak Concentrations and Arrival Times at the Core Zone Boundary for Uranium-238. Relative peaks and arrival time differences are with respect to the base case (no additional flux).

Case	Peak Concentration (pCi/L)	Arrival Time (yr)	Relative Peak	Arrival Time Difference
No Additional Flux	5.99	2280	–	–
16,000 Acre-ft/yr	8.54	2108	1.43	-171
27,000 Acre-ft/yr	9.03	2088	1.51	-191

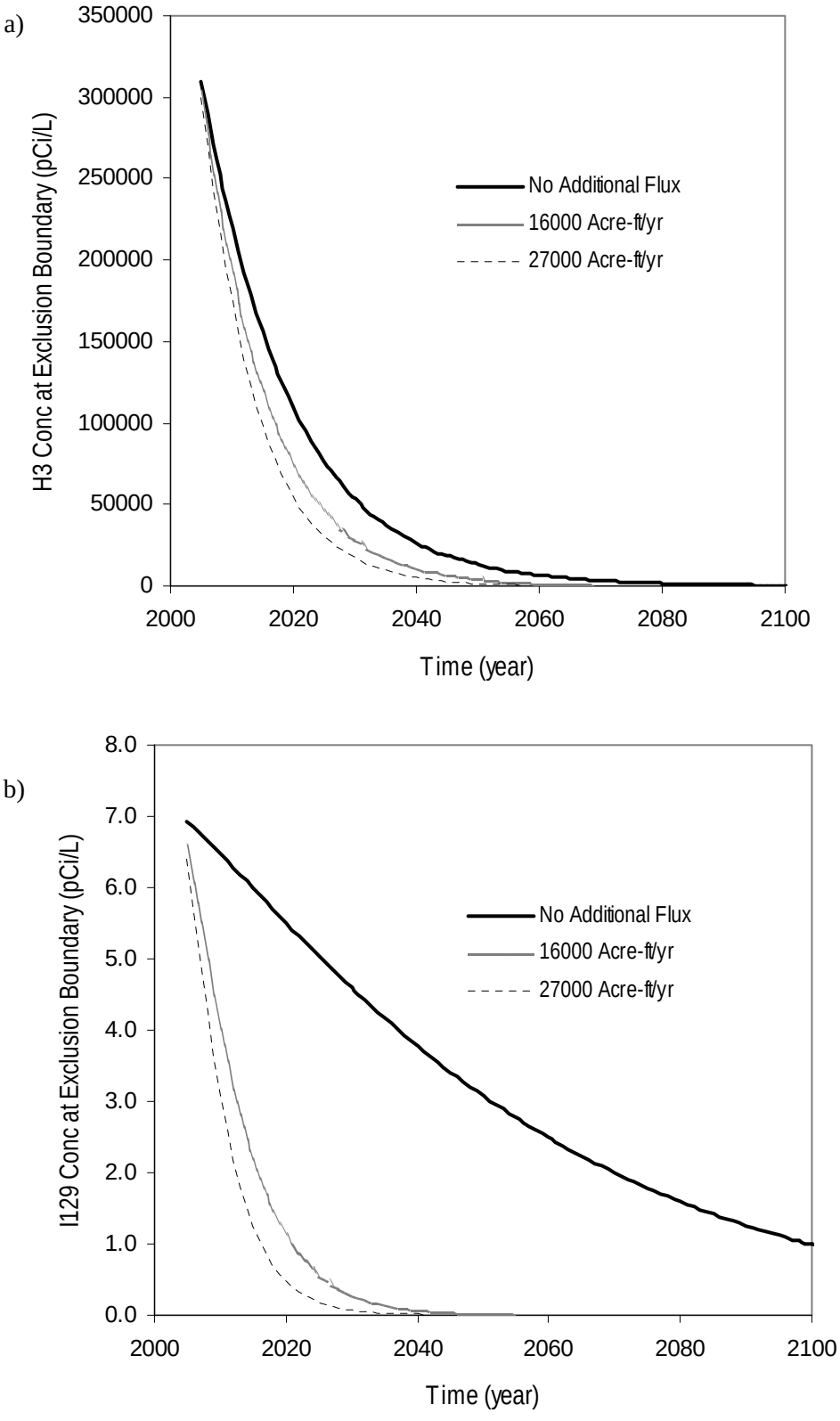

Figure 4.4. Concentration Versus Time at Peak Locations on the Core Zone Boundary for a) Tritium and b) Iodine-129

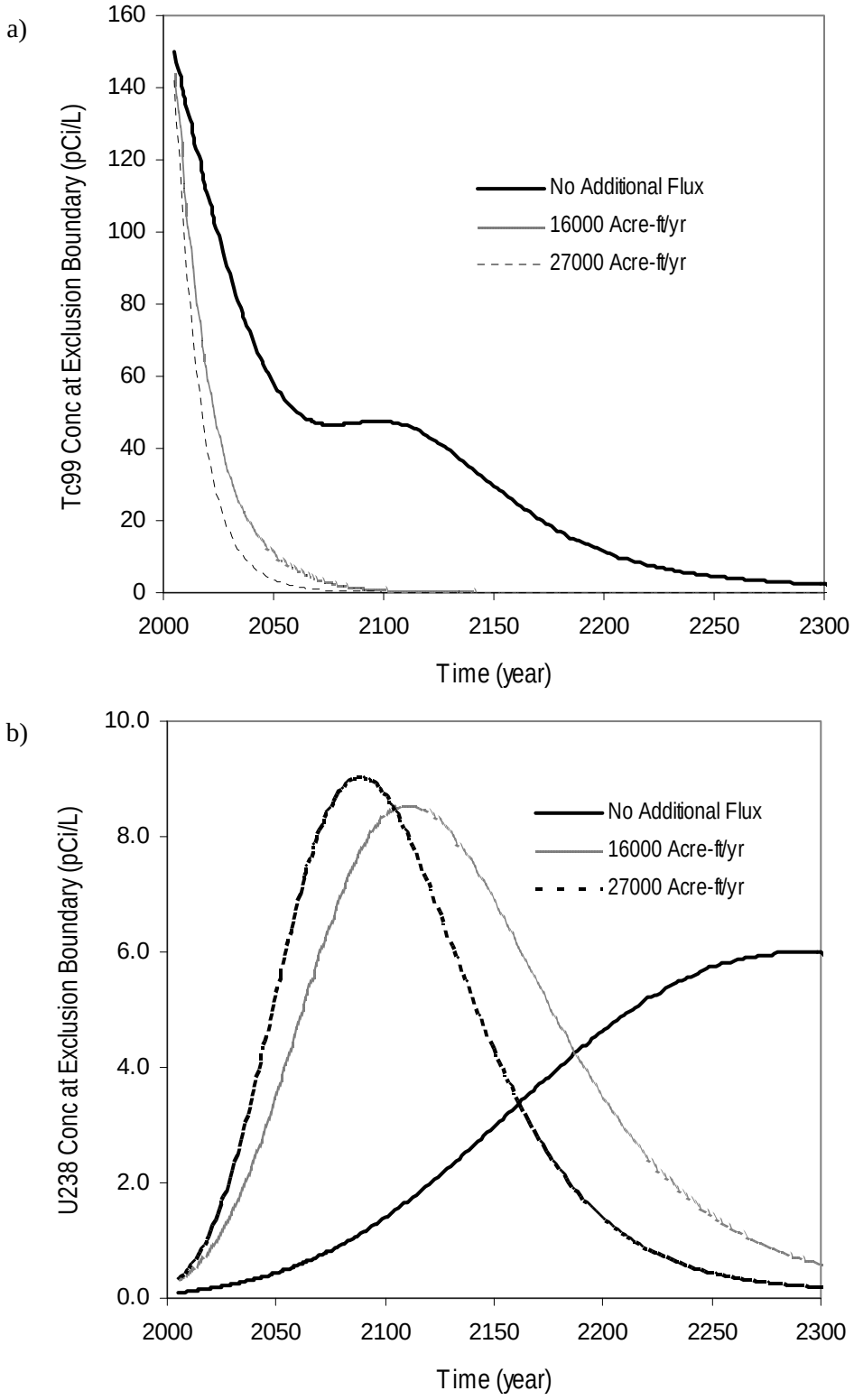

Figure 4.5. Concentration Versus Time at Peak Locations on the Core Zone Boundary for a) Technetium-99 and b) Uranium-238

potential flux increase was in accelerating the transport of the contaminants out of the core zone. This effect was most significant with iodine-129, where concentrations dropped below the DWS within 20 years for the additional flux cases. For the base case, however, more than 100 years was required for the concentration to drop below the DWS.

Because uranium-238 is strongly sorbed to sediments, its estimated concentration distribution in the year 2005 is far less dispersed than the other more mobile contaminants (Figure 4.2). Peak concentrations also occurred later in the simulation and increased with the magnitude of the upland boundary flux. Despite increases in peak concentrations, the peak did not exceed the DWS in any of the three flow cases. Further evidence of the accelerated transport was noted in the peak arrival times, which were 171 years for the 16,000 acre-ft/yr case and 191 years for the 27,000 acre-ft/yr case.

4.1.1.2 Results at the Columbia River

Tables 4.5 through 4.8 report the peak concentrations and arrival times at the Columbia River for each of the contaminants. Also reported in these tables are their relative peak concentrations and differences in arrival times. What is not fully evident from the tabulated data is that higher upland fluxes tended to initially increase contaminant concentrations but then experience a more rapid decline than the base case (no additional flux). For example, breakthrough curves for all contaminants are shown in Figures 4.6 and 4.7. For both tritium (Figure 4.6a) and technetium-99 (Figure 4.7a), higher peaks occurred that were accelerated with respect to the base case. For the technetium-99, this occurred on the second peak of the double-peaked breakthrough curve.

Although increases in the upland fluxes accelerated contaminant transport to the river, this impact was not significant for technetium-99 and tritium. Concentrations of technetium-99 at the Columbia River were well below the DWS of 900 pCi/L. For tritium, the DWS was exceeded in the base case until ~2027. For the highest flux case (27,000 acre-ft/yr), the concentration dropped below the DWS at ~2022.

Breakthrough curves for iodine-129 transport demonstrate that concentrations dropped below the DWS ~2075 for the base case, and ~2015 for the additional flux cases. Although the magnitude of the upland flux differed for the two additional flux cases, for iodine-129, only minor differences were observed in the breakthrough curves (Figure 4.6a). This result was also similar to tritium transport behavior. Because both contaminant distributions were initially dispersed with high-concentration zones outside the core zone, the difference in the effects of the two upland flux values was minimal.

Figure 4.7b shows that the peak uranium-238 concentration at the Columbia River had only been attained by the highest flux case. Concentrations for the 16,000 acre-ft/yr case were still increasing, but did not differ significantly from the 27,000 acre-ft/yr case. By contrast, the concentrations for the base case were so low relative to the others that the concentrations plotted along the x-axis. As noted in Table 4.8, although true peaks were never attained, concentrations were several hundred times higher in the additional flux cases than in the base case. Despite the accelerated transport, uranium concentrations (~0.3 pCi/L) were well below the DWS of 27 pCi/L.

Table 4.5. Peak Concentrations and Arrival Times at the Columbia River for Tritium. Relative peaks and arrival time differences are with respect to the base case (no additional flux).

Case	Peak Concentration (pCi/L)	Arrival Time (yr)	Relative Peak	Arrival Time Difference
No Additional Flux	66,700	2005	–	–
16,000 Acre-ft/yr	72,900	2007	1.09	+2
27,000 Acre-ft/yr	79,300	2007	1.19	+2

Table 4.6. Peak Concentrations and Arrival Times at the Columbia River for Iodine-129. Relative peaks and arrival time differences are with respect to the base case (no additional flux).

Case	Peak Concentration (pCi/L)	Arrival Time (yr)	Relative Peak	Arrival Time Difference
No Additional Flux	7.83	2005	–	–
16,000 Acre-ft/yr	6.94	2005	0.89	0
27,000 Acre-ft/yr	6.58	2005	0.84	0

Table 4.7. Peak Concentrations and Arrival Times at the Columbia River for Technetium-99. Relative peaks and arrival time differences are with respect to the base case (no additional flux).

Case	Peak Concentration (pCi/L)	Arrival Time (yr)	Relative Peak	Arrival Time Difference
No Additional Flux	178	2005	–	–
16,000 Acre-ft/yr	178	2005	1.0	0
27,000 Acre-ft/yr	177	2005	0.99	0

Table 4.8. Peak Concentrations and Arrival Times at the Columbia River for Uranium-238. Relative peaks and arrival time differences are with respect to the base case (no additional flux).

Case	Peak Concentration (pCi/L)	Arrival Time (yr)	Relative Peak	Arrival Time Difference
No Additional Flux	7.28E-04	2305	–	–
16,000 Acre-ft/yr	2.75E-01	2305	378[(a)]	[(a)]
27,000 Acre-ft/yr	3.68E-01	2278	505[(a)]	[(a)]
(a) Peak occurred at end of simulation (true peak did not occur).				

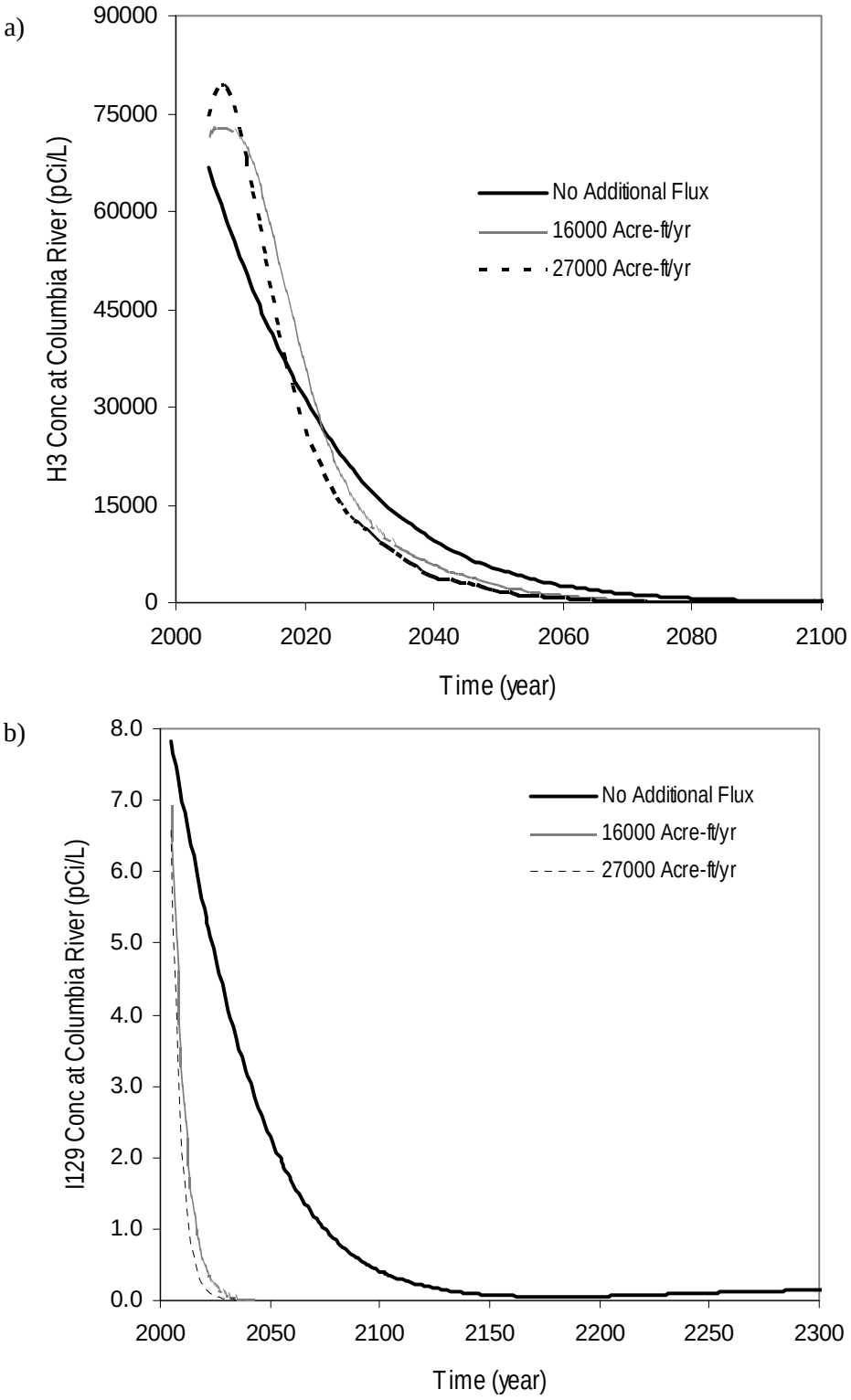

Figure 4.6. Concentration Versus Time at Peak Locations on the Columbia River for a) Tritium and b) Iodine-129

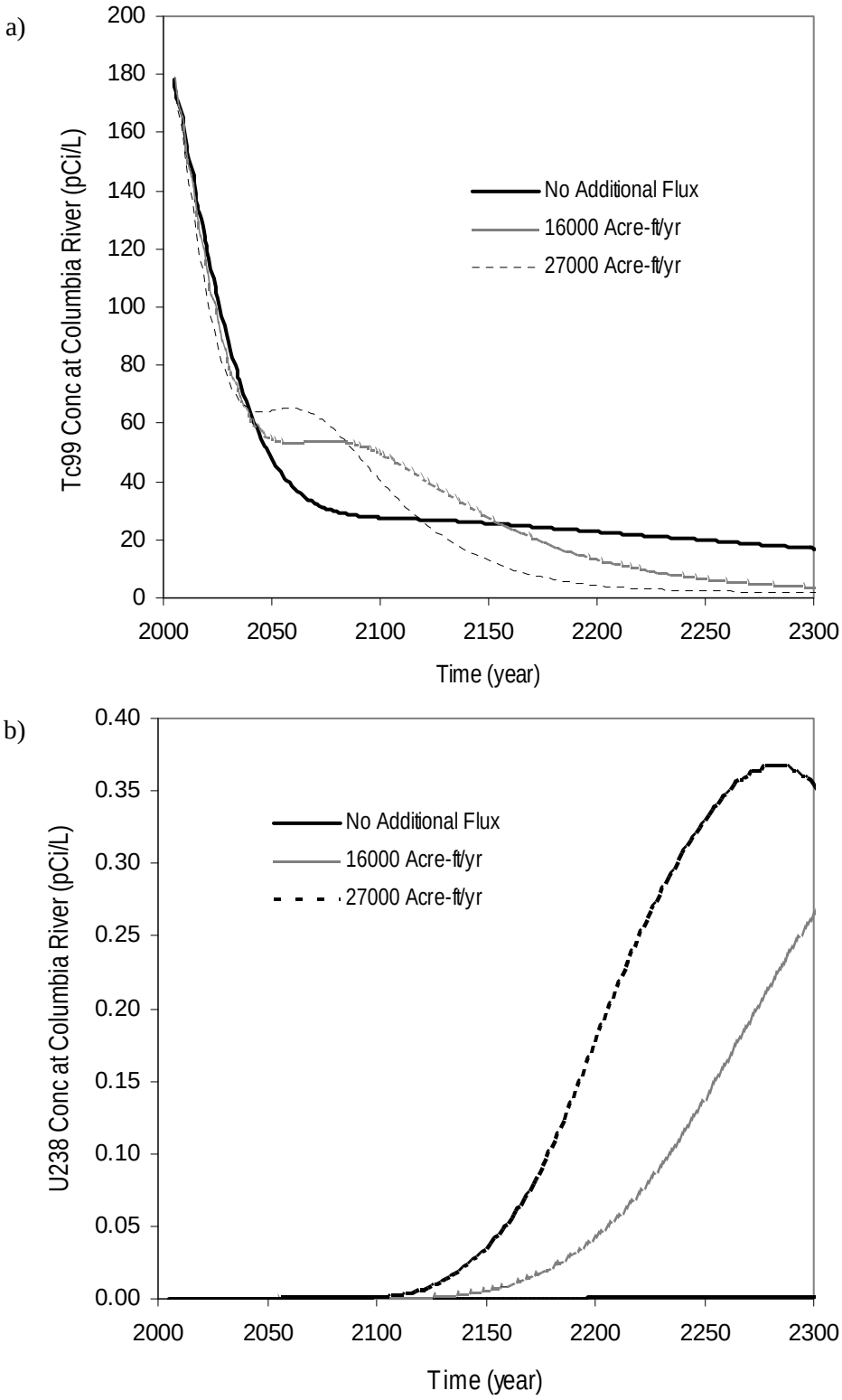

Figure 4.7. Concentration Versus Time at Peak Locations on the Columbia River for a) Technetium-99 and b) Uranium-238

4.1.2 Contaminated Area of the Aquifer at the DWS

Although peak concentrations are useful for identifying concentration limits at the selected boundaries, quantifying the area of the aquifer contaminated at or above the DWS demonstrates the impact the upland fluxes may have on a Site-wide basis. Impacts to the tritium and iodine-129 plumes were of particular interest given that it is assumed that these plumes between the core zone and Columbia River will exceed the DWS for the next 150 to 300 years (DOE 2005).

Figures 4.8 and 4.9 plot the area of the aquifer contaminated at or above the DWS with time. The radionuclides that exceeded DWS over the largest area were tritium (<20 km^2) and iodine (< 7 km^2) due to their widespread concentration distribution in the subsurface simulation. By contrast, the DWS for technetium-99 (<0.12 km^2) and uranium-238 (0.03 km^2) were exceeded only in the high-concentration zones shown in Figure 4.2.

Similar to peak concentration behavior at the Columbia River, the additional flux at the upland boundary initially increased the area of the aquifer contaminated at or above the tritium DWS, then experienced a sharper decline relative to the base case. By the year 2045, the area of the aquifer contaminated at or above the tritium DWS was near zero for the additional flux cases. This point was reached in the base case only five years later. In all cases, the contamination was widespread and was found both inside and outside the core zone (see Figure 4.1).

For iodine-129, the effect on groundwater concentrations was more significant. By 2300, the contaminated area at or above the DWS had not yet been reached. For the 16,000 acre-ft/yr case, the contaminated area approached zero ~2300, and for the 27,000 acre-ft/yr case, ~2250. The contaminated area lay principally in the areas between the core zone and the Columbia River, both north and east of Gable Gap (see Figure 4.1).

The uranium-238 contaminant plume showed similar behavior with respect to the area of the aquifer contaminated at or above the DWS. The contaminated area was initially increased with the higher flux cases, but then decreased more rapidly than the base case. This area approached zero in the year ~2050 for the highest flux case, ~2060 for the intermediate flux value, and ~2150 for the base case (no additional flux). For all three flow fields, the contamination was confined to a very small area in the core zone.

The technetium-99 plume demonstrated different behavior, with the base case consistently predicting a smaller contaminated area relative to the higher flux cases. The highest flux (27,000 acre-ft/yr) predicted the highest contaminated area. Given that the area of the aquifer contaminated at or above the DWS was confined to the high-concentration zones (Figure 4.2), the base case (no additional flux) caused less spreading of the plume. At higher fluxes, the plume was transported more rapidly, causing a larger area to be contaminated at or above the DWS.

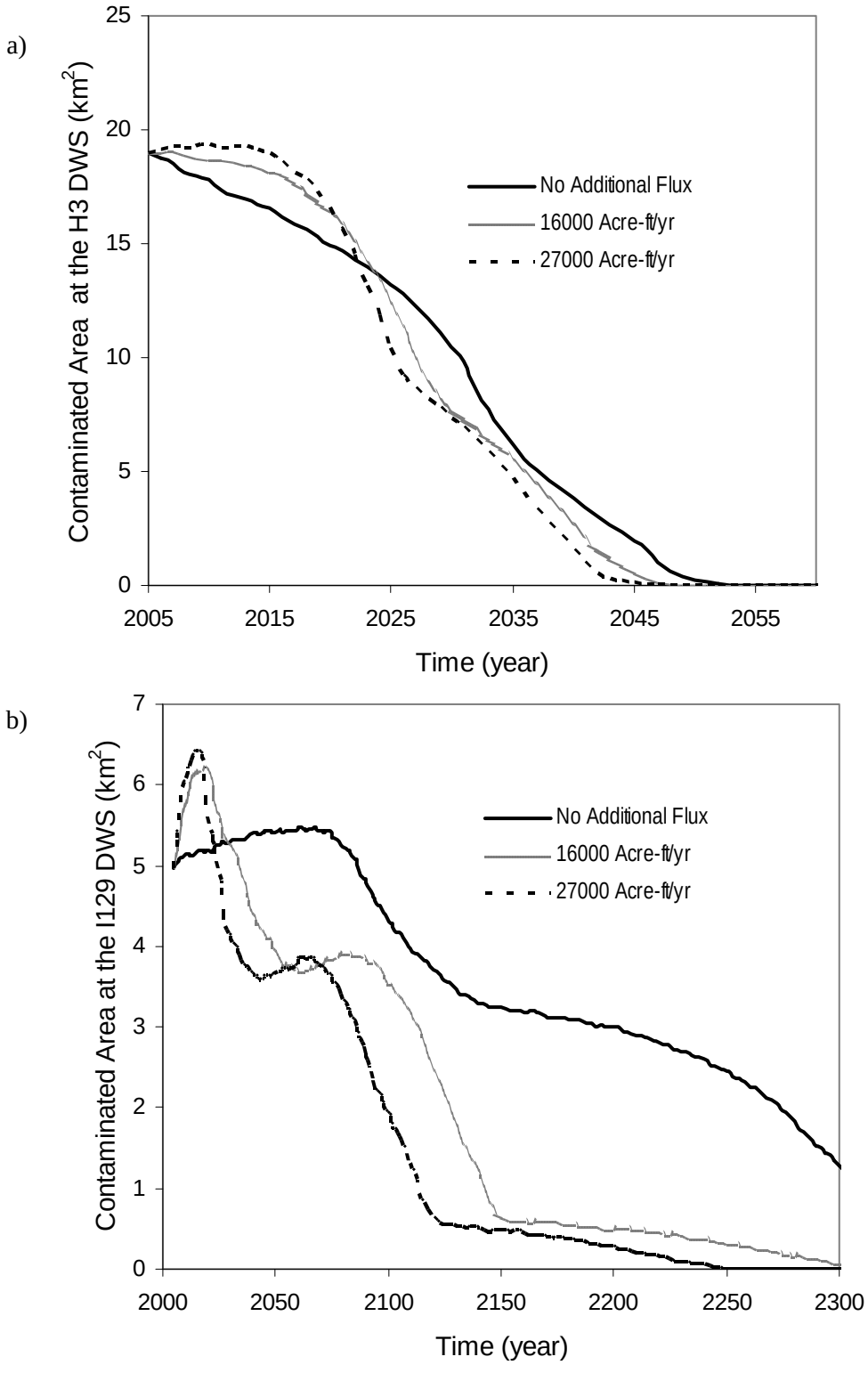

Figure 4.8. Area of Aquifer Contaminated at or Above the DWS for a) Tritium and b) Iodine-129

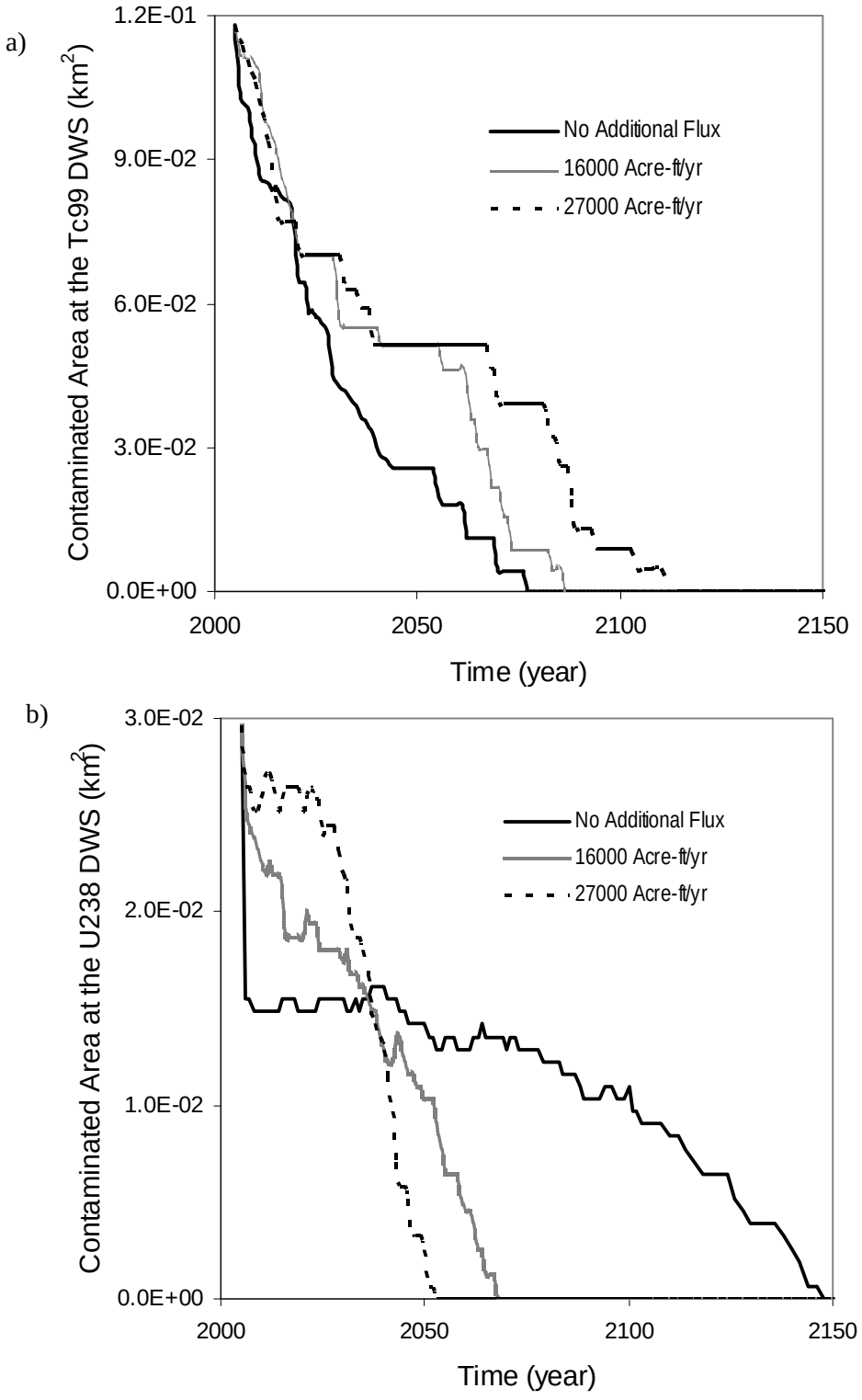

Figure 4.9. Area of Aquifer Contaminated at or Above the DWS for a) Technetium-99 and b) Uranium-238

4.1.3 Contaminated Area of the Aquifer at 10 Times the DWS

The area of the aquifer contaminated at or above ten times the DWS was also analyzed for the three different flow fields. Tritium, however, was the only contaminant that exceeded 10 times the DWS (Figure 4.10). Only small differences in the contaminated area existed among the three different flow fields. The base case contaminated area approached zero ~2015, whereas this occurred a few years earlier for the higher-flux cases. Only small differences in the contaminated area existed among the various cases, with the base case consistently predicting a larger contaminated area than the other two cases.

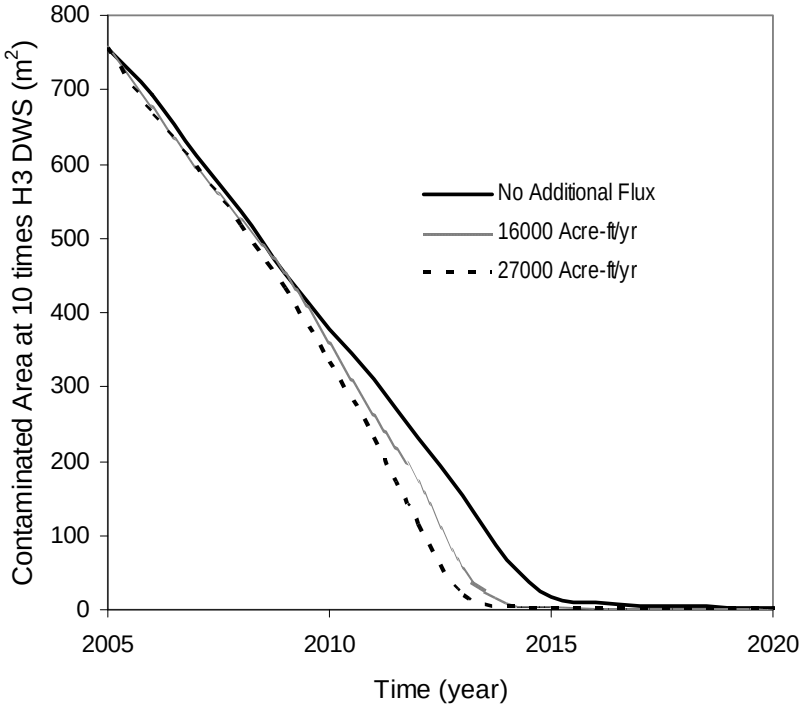

Figure 4.10. Area of Aquifer Contaminated at or Above 10 Times the DWS for Tritium

4.1.4 Total Activity

The total activity remaining at the end of the simulation was also examined for each of the radionuclides and all three flow scenarios. Results of this analysis are plotted in Figure 4.11, which shows the total activity remaining in the simulation domain in the year 2305 relative to the base case. In general, the increase in the upland fluxes caused more mass to discharge to the Columbia River. For the more mobile contaminants (tritium, technetium-99, and iodine-129), the 16,000 acre-ft/yr flux case, on average, transported 58% more mass to the boundaries. For the 27,000 acre-ft/yr flux case, this average was 67%. Even though more mass discharged into the Columbia River, the peak concentration analysis demonstrated that concentrations were diluted with respect to the base case. Concentrations for the higher-flux cases experienced slightly higher peaks at earlier times but decreased concentrations at later times.

For uranium-238, only small differences in the total activity remaining in the domain resulted for each of the three flow cases. Because uranium-238 is strongly sorbed, its transport was retarded with respect to the more mobile contaminants.

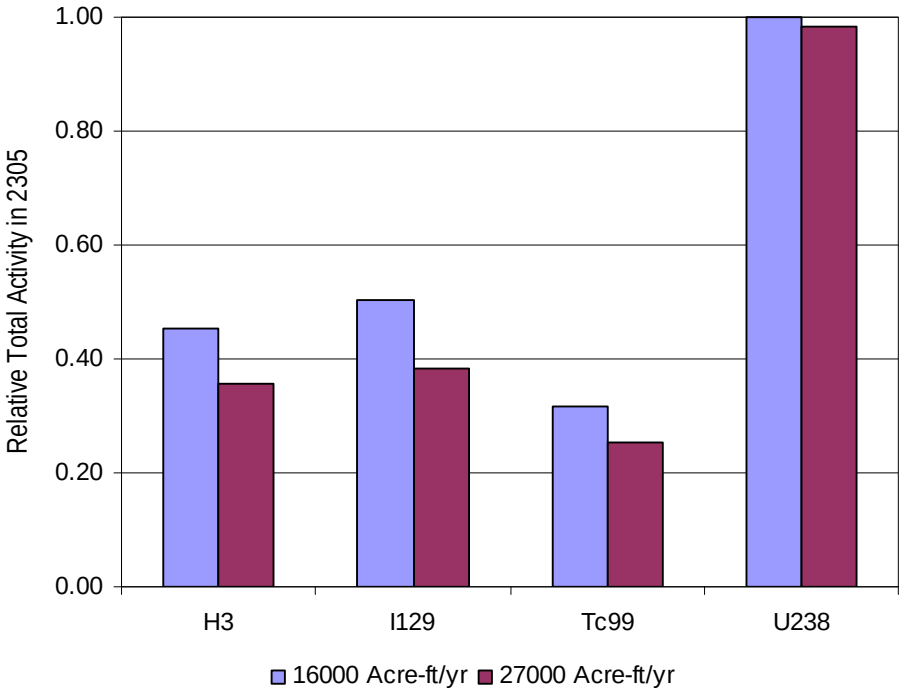

Figure 4.11. Relative Total Activity of Radionuclides at the End of the Simulation (Year 2305)

4.2 Unit Source Analysis

Unit source releases were also simulated for a hypothetical tracer (i.e., no retardation and no decay). The objectives of this analysis were to 1) assess the temporal changes in the areal extent of the plume when no solute was initially present, and 2) determine travel times to the boundaries for each of the three flow fields. Two simulations were executed for each flow field, one in which the source originated from a central location in 200 West and another in which the source originated from a central location in 200 East.

4.2.1 Areal Extent of Plume

All three of the steady-state flow fields in this analysis predicted that groundwater flowed northward from the Central Plateau through Gable Gap and discharged to the northern reach of the Columbia River. Consistent with field observations, the initial concentration distributions shown in Figures 4.1 and 4.2 depict that groundwater mounds caused both easterly and northerly flows from the Central Plateau. There is uncertainty about the future predominant flow direction because of the uncertainty in the top of basalt elevation in the gap. If the water table declines below the top of basalt, northward flow could be cut off through the gap.

The aquifer area north of Gable Gap is small relative to the potential flow area south of the gap. In the initial concentration distribution analysis, all of the contaminants except uranium-238 had already been transported north of Gable Gap at the start of the transient transport simulations. For this reason, a

qualitative assessment of the areal extent of the contaminant plumes was performed because no contaminant was present in the simulation domain at the start of the simulation.

Plumes from both 200 Areas discharged in the same general area of the Columbia River. Shown in Figure 4.12 are the unit source results for the 200 West Area at the year where maximum areas of the contaminant plume were attained. As noted by the years in the figures, differences in flow velocities resulted in the maximum area being attained at different times. Consistent with the theoretical expectation, the maximum area for the base case is attained ~150 years later than the highest recharge case and ~65 years later than the intermediate estimate. Although the areal extent of the contaminant plume is largest for the base case and smallest for the highest flux case, these differences are small and would have little effect on contaminant plume migration.

4.2.2 Travel Times

Results of the 300-year time-dependent transport for the six simulations are shown in Figure 4.13, which reports relative peaks and arrival times for each of the solutes. While the bars in Figure 4.13 represent peak concentrations relative to the base case, the label attached to each bar reports the difference in arrival times. In all cases, travel times were accelerated to the downstream boundaries, with only small differences in travel times resulting for the 16,000 and 27,000 acre-ft/yr flux cases. A source from 200 West, on average, was transported to the core zone 62.5 years earlier than in the base case. From 200 East, the travel time to the core zone was accelerated an average 4.5 years. Travel times to the Columbia River were more significantly affected by differences in the flow fields. From 200 West, the average travel time was accelerated by 166.5 years and from 200 East by 96 years.

a)

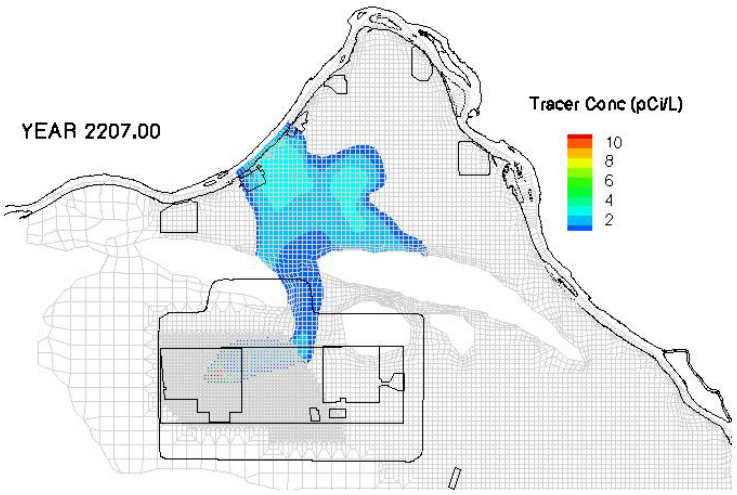

b)

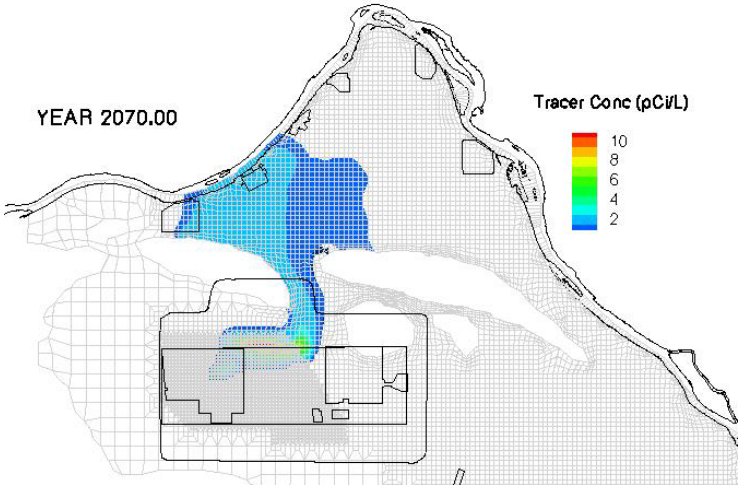

c)

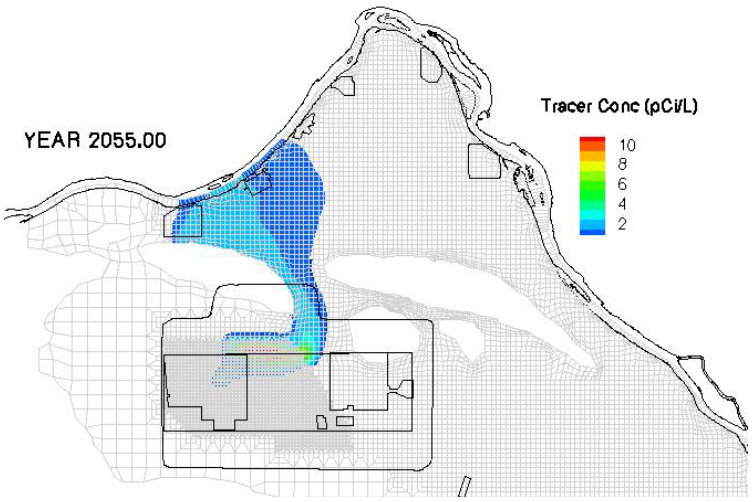

Figure 4.12. Qualitative Comparison of the Areal Extent of the Tracer Plume for a) Base Case, b) Intermediate Flux Case (16,000 acre-ft/yr), and c) Maximum Flux Case (27,000 acre-ft/yr)

Figure 4.13. Relative Peak Concentrations and Arrival Times at Downstream Boundaries. Bars represent relative peaks, whereas label refers to relative arrival time.

5.0 Summary and Preliminary Conclusions

Initial scoping calculations that assessed the potential hydrologic effects of the proposed Black Rock Reservoir on the Hanford unconfined aquifer were studied in this investigation. Although results of the numerical simulations were analyzed quantitatively with respect to the DWS, results should be interpreted as a qualitative assessment of impacts given the simplifying assumptions used in this initial analysis. For example, steady-state flow analyses were used to obtain an initial assessment of flow, as well as an initial estimate of maximum recharge previously observed in certain locations in the Hanford unconfined aquifer. The steady-state flow field analysis did not consider effects on current groundwater mounds beneath the 200 Areas in the Central Plateau, which could be addressed with a transient flow analysis.

Simulated estimates of contaminant distributions were used in this analysis because they were adequate for assessing relative impacts for the three different flow fields. The transient transport analyses demonstrated that increases in lateral recharge resulted in faster contaminant travel times. Of particular concern was the potential mobilization of contaminants in the vadose zone. This potential impact, however, was not considered in this initial study, but could be addressed with a saturated-unsaturated flow and transport analysis.

Because the maximum recharge that was determined in the first part of this investigation is only an estimate, the hydrologic impact assessment on contaminant transport should also be viewed as preliminary. After the USBR has completed a quantitative analysis of the potential recharge from the proposed Black Rock Reservoir, an evaluation of the potential hydrologic impacts to the Hanford Site unconfined aquifer system should be reexamined. In addition to more quantitative recharge estimates, the hydraulic conductivity distributions within Dry Creek need to be reexamined. This is demonstrated by the water-table predictions at Dry Creek, which show the potential for perennial surface flow at this location. Once a better understanding of the groundwater-surface water flow conditions within Dry Creek are obtained, a maximum lateral recharge can be estimated based on the surface elevation at Dry Creek.

Despite the limitations imposed by the simplifying assumptions, several important results were demonstrated by this study. For example, results showed that increases in the lateral recharge had limited impact on regional flow directions but accelerated contaminant transport. Although contaminant concentrations may have initially increased for the more mobile contaminants (tritium, technetium-99, and iodine-129), the accelerated transport caused dilution and a more rapid decline in concentrations relative to the base case (no additional flux). For the low-mobility uranium-238, higher lateral recharge caused increases in concentration, but these concentrations never approached the DWS.

In this preliminary investigation, contaminant concentrations did not exceed the DWS study metric. With the increases in upland fluxes, more mass was transported out of the aquifer, and concentrations were diluted with respect to the base case. More specific impacts on flow and transport are summarized in the following sections.

5.1 Impacts on Groundwater Flow

An analysis of the three flow fields showed that regional flow directions were largely unaffected by the increase in the upland boundary fluxes. The primary effect was on flow velocities, which increased with the steeper gradient associated with the higher fluxes. The areas affected most by changes in the flux were the Central Plateau and the area east of Rattlesnake Hills. In these areas, flow velocities in the Hanford formation were 10 to 100 times higher in the additional flux cases relative to the base case.

5.2 Hypothetical Impacts on Contaminant Transport

Results of the contaminant transport analysis consistently demonstrated that increases in upland boundary fluxes accelerated contaminant transport. This result was also observed by examining the total activity in the domain remaining at the end of the simulation. For the more mobile contaminants (tritium, technetium-99, and iodine-129), the 16,000 acre-ft/yr flux case, on average, transported 58% more mass to the boundaries. For the 27,000 acre-ft/yr flux case, this average was 67%. For uranium-238, only small differences resulted in the total activity remaining in the domain for each of the three flow cases.

5.2.1 Core Zone

At the core zone, the primary impact from the potential fluxes was the acceleration of transport out of the core zone. For the more mobile contaminants, tritium, technetium-99, and iodine-129, the increased upland fluxes caused contaminant concentrations to dilute with respect to the base case. This impact was most significant with iodine-129, where concentrations dropped below the DWS within 20 years for the additional flux cases. For the base case, however, more than 100 years was required for the concentration to drop below the DWS.

The increased fluxes also accelerated transport of uranium-238. However, for this low-mobility contaminant, peak concentrations increased with the magnitude of the upland boundary flux and accelerated their arrival times. Despite increases in peak concentrations, concentrations did not even approach the DWS in any of the three flow cases.

5.2.2 Columbia River

The transport analysis showed that the primary effect on the Columbia River was to accelerate contaminant migration. This effect was insignificant for both technetium-99 and uranium-238 because their concentrations remained well below the DWS for all three flow cases. Effects on tritium concentrations at the river were also insignificant. For all three flow fields, concentrations at the river dropped below the DWS within the same five-year period (~2025). The most significant effect at the river was with the iodine-129 plume. Iodine-129 concentrations at the river were significantly diluted in the higher flux cases, causing concentrations to drop below the DWS ~60 years earlier than in the base case (no additional flux).

5.2.3 Area Contaminated at or Above the DWS

With the exception of technetium-99, the area of the aquifer contaminated at or above the DWS was initially higher in the additional flux cases, then decreased more rapidly than the base case. After 20 years of simulation, the contaminated area of the aquifer was highest for the base case for uranium-238, tritium, and iodine-129. For uranium-238, the contaminated area was confined to a very small area in the core zone. For iodine-129 and tritium, the contaminated area at or above the DWS lay principally in the areas between the core zone and the Columbia River, both north and east of Gable Gap.

The technetium-99 plume demonstrated different behavior. The base case consistently predicted a smaller contaminated area relative to the higher flux cases. The highest flux (27,000 acre-ft/yr) predicted the highest contaminated area. The area of the aquifer contaminated at or above the DWS was confined to the high-concentration zones shown in Figure 4.2.

5.2.4 Travel Times

In all cases, travel times were accelerated to the downstream boundaries, with only small differences in travel times resulting for the 16,000 and 27,000 acre-ft/yr flux cases. A source from the 200 West Area, on average, was transported to the core zone 62.5 years earlier than in the base case. From 200 East, the travel time to the core zone was accelerated an average 4.5 years. Travel times to the Columbia River were more significantly affected by differences in the flow fields. From 200 West, the average travel time was accelerated by 166.5 years and from 200 East by 96 years.

6.0 References

Bryce RW, CT Kincaid, PW Eslinger, and LF Morasch (Eds.). 2002. *An Initial Assessment of Hanford Impact Performed with the System Assessment Capability*. PNNL-14027, Pacific Northwest National Laboratory, Richland, Washington.

Cole CR, SK Wurstner, MP Bergeron, MD Williams, and PD Thorne. 1997. *Three–Dimensional Analysis of Future Groundwater Flow Conditions and Contaminant Plume Transport in the Hanford Site Unconfined Aquifer System: FY 1996 and 1997 Status Report*. PNNL-11801, Pacific Northwest National Laboratory, Richland, Washington.

Cole CR, MP Bergeron, SK Wurstner, PD Thorne, S Orr, and MI McKinley. 2001. *Hanford Site-Wide Groundwater Model Calibration Using Inverse Methodology*. PNNL-13447, Pacific Northwest National Laboratory, Richland, Washington.

Eslinger PW, CT Kincaid, WE Nichols, and SK Wurstner. 2006. *A Demonstration of the System Assessment Capability, Rev. 1 Software for Hanford Remediation Assessment Project*. PNNL-16209, Pacific Northwest National Laboratory, Richland, Washington.

Freedman VL, Y Chen, and SK Gupta. 2005a. *CFEST Coupled Flow, Energy & Solute Transport Version CFEST005 Theory Guide*. PNNL-15452 Rev. 1, Pacific Northwest National Laboratory, Richland, Washington.

Freedman VL, ZF Zhang, SR Waichler, and SK Wurstner. 2005b. *2005 Closure Assessments for WMA-C Tank Farms: Numerical Simulations*. PNNL-15377, Pacific Northwest National Laboratory, Richland, Washington.

Freedman VL, Y Chen, A Gilca, CR Cole, and SK Gupta. 2006. *CFEST Coupled Flow, Energy & Solute Transport Version CFEST005 User's Guide*. PNNL-15915 Rev. 1, Pacific Northwest National Laboratory, Richland, Washington.

Hanford Future Site Uses Working Group (HFSUWG). 1992. *The Future for Hanford: Uses and Cleanup*. Westinghouse Hanford Company, Richland, Washington.

Hartman MJ, LF Morasch, and WD Webber (Eds.). 2006. *Hanford Site Groundwater Monitoring for Fiscal Year 2005*. PNNL-15670, Pacific Northwest National Laboratory, Richland, Washington.

Kincaid CT, RW Bryce, and JW Buck. 2004. *Technical Scope and Approach for the 2004 Composite Analysis of Low Level Waste Disposal at the Hanford Site*. PNNL-14372, Pacific Northwest National Laboratory, Richland, Washington.

Newcomb RC, JR Strand, and FJ Frank. 1972. *Geology and Ground-Water Characteristics of the Hanford Reservation of the U.S. Atomic Energy Commission, Washington.* Geological Survey Professional Paper 717, U.S. Geological Survey, Washington, D.C.

Newcomer DR, PD Thorne, and PE Dresel. 1998. "Hanford Groundwater Monitoring Project." *Hanford Site Environmental Report for Calendar Year 1997*. PNNL-11795, Pacific Northwest National Laboratory, Richland, Washington.

Thorne PD, MP Bergeron, MD Williams, and VL Freedman. 2006. *Groundwater Data Package for Hanford Assessments*. PNNL-14753 Rev. 1, Pacific Northwest National Laboratory, Richland, Washington.

U.S. Department of Energy (DOE). 1999. *Final Hanford Comprehensive Land-Use Plan Environmental Impact Statement*. DOE/EIS-0222-F, DOE Richland Operations Office, Richland, Washington.

U.S. Department of Energy (DOE). 2005. *Hanford Site End-State Vision.* DOE/RL-2005-57, DOE Richland Operations Office, Richland, Washington.

Vermeul VR, CR Cole, MP Bergeron, PD Thorne, and SK Wurstner. 2001. *Transient Inverse Calibration of Site-Wide Groundwater Model to Hanford Operational Impacts from 1943 – 1996 – Alternative Conceptual Model Considering Interaction with Uppermost Basalt Confined Aquifer*. PNNL-13623, Pacific Northwest National Laboratory, Richland, Washington.

Vermeul VR, MP Bergeron, CR Cole, CJ Murray, WE Nichols, TD Scheibe, PD Thorne, SR Waichler, and Y Xie. 2003. *Transient Inverse Calibration of the Site-Wide Groundwater Flow Model (ACM-2): FY03 Progress Report*. PNNL-14398, Pacific Northwest National Laboratory, Richland, Washington.

Waichler SR, MS Wigmosta, and A Coleman. 2004. *Natural Recharge to the Unconfined Aquifer System on the Hanford Site from the Greater Cold Creek Watershed: Progress Report 2004*. PNNL-14717, Pacific Northwest National Laboratory, Richland, Washington.

Washington State Department of Ecology, U.S. Environmental Protection Agency, and U.S. Department of Energy. 1989. *Hanford Federal Facility Agreement and Consent Order*, as amended (the Tri-Party Agreement). Ecology, EPA, and DOE, Olympia, Seattle, and Richland, Washington.

Zhang ZF, VL Freedman, and SR Waichler. 2004. *2004 Initial Assessments for the T and TX TY Tank Farm Field Investigation Report (FIR): Numerical Simulations*. PNNL-14838, Pacific Northwest National Laboratory, Richland, Washington.

Distribution

No. of Copies

OFFSITE

15 U.S. Bureau of Reclamation

K. Didriksen
U.S. Bureau of Reclamation
PO Box 620
Grand Coulee, WA 99133

ONSITE

4 U.S. Department of Energy

K. M. Thompson	A6-38
J. G. Morse	A6-38
B. L. Charboneau	A6-33
T. W. Ferns	A5-15

5 Pacific Northwest National Laboratory

V. L. Freedman	K9-36
F. Spane	K6-96
S. R. Waichler	K9-36
Information Release (2)	P8-55